The University of Manitoba

REVERSE DESCRIBING FUNCTION

by

Ian Douglas Walkty

A Thesis

Submitted to the Faculty of Graduate Studies

in Partial Fulfilment of the Requirements for the Degree

Master of Science

DEPARTMENT OF ELECTRICAL ENGINEERING

Winnipeg, Canada

October, 1973

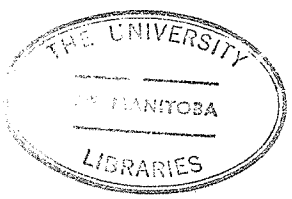

ABSTRACT

The Reverse DF is introduced as a means of effectively analyzing nonlinear, closed loop systems possessing a high pass linear plant, and hence significant harmonic components in the feedback signal. The technique is applied to single-valued, zero-memory, time invariant nonlinearities. The major restriction is to non-zero sloped nonlinearities over a non-finite input range. This reverse approach is applied to the DF, the rms DF, and the DIDF with a high degree of success. The Pattern Search of Hooke and Jeeves is used to solve the resulting simultaneous nonlinear DIDF equations. Jump phenomena predictions are also investigated, with considerable success for both a sinusoidally forced high pass system and a low pass system forced by a triangular waveform.

TABLE OF CONTENTS

(TABLE OF CONTENTS - continued)

LIST OF FIGURES

(LIST OF FIGURES - continued)

LIST OF TABLES

ACKNOWLEDGEMENTS

This thesis could not have been finished without the support and inspiration of several individuals. The National Research Council and the University of Manitoba provided the financial assistance. My advisor, Professor R.A. Johnson, provided moral and technical assistance. His continuous, and yet subtle guidance will long be remembered. Thanks are also extended to my parents and to Kathy, whose encouragement made this completion possible.

CHAPTER 1

INTRODUCTION

The idea of the describing function (DF) cannot be attributed to a single person, as it was almost simultaneously introduced by R.J. Kochenburger, A. Tustin, W. Oppelt, L.C. Goldfarb, and J. Dutilh [1 p. 49] around 1950. This method has become widely accepted in the study of oscillations in autonomous (time invariant and unforced) nonlinear systems, and may be applied to a wide variety of nonlinearities including continuous and discontinuous, single-valued or with hysteresis. The popularity of this approximation is undoubtedly attributed to the simplicity of its use, as well as to its generality. The DF method may currently be applied with some degree of confidence only to low pass systems (Sec. 3.1). The purpose of this thesis is to develop an approach to studying oscillations in a system whose linear plant is not low pass. This approach would widen the scope of application of the DF by removing in certain cases one of its major restrictions viz. the low pass assumption.

1.1 PRACTICAL CONSIDERATIONS

This thesis will deal with the basic autonomous, nonlinear, time invariant feedback system shown in Fig. 1.1. The forward path consists of one single-valued nonlinearity

followed by a linear plant, while the negative feedback path has unity gain.

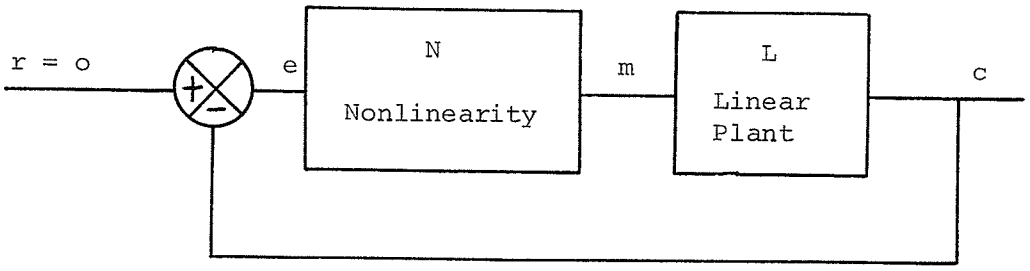

Fig. 1.1

GENERAL AUTONOMOUS NONLINEAR SYSTEM

In the conventional DF approach, the input to the nonlinearity, e, is assumed to be a sinusoid. Due to the characteristic behaviour of the nonlinearity, the output m will contain the frequency of the input and its harmonics. A ~~necessary~~ normally applied condition of the DF method, the filter hypothesis (Sec. 3.1), is now invoked. This means that the (low pass) linear plant essentially filters out the harmonics in m . Therefore, the signal in the feedback loop is nearly sinusoidal, which justifies the original assumption of the waveform of e . This DF approximation yields accurate results in many cases, although it sometimes fails when it is expected to work, or works extremely well when it is expected to fail [1 p.162]. If the linear plant were high pass instead of low pass, the harmonics inherent in m would be amplified and the

feedback signal would be highly distorted. In this case, the sinusoidal approximation of e is very poor and predictions based on the DF would be expected to be poor.

In the high pass case, the sinusoidal approximation should be made at m. Signal balance is achieved by taking m through the nonlinearity to e, and m through the linear plant to c, and equating c and -e. The signal at c will be sinusoidal and -e will contain the frequency of m and its harmonics. Because the high pass plant is no longer a source of harmonic distortion, the predictions based on the sinusoidal approximation at m are expected to be good. This approach will be referred to as the reverse method while the conventional DF approach will be termed the direct method.

This reverse method may be interpreted mathematically in another sense. The sinusoidal approximation is made at m and the signal-flow is assumed in a counter-clockwise direction. This means e will contain the frequency of m and its harmonics, and the linear transfer function will be inverted. Hence, what was originally a high pass linear plant is now low pass (Sec. 1.1.2). This linear plant filters out the harmonics in -e and the signal present at m is essentially sinusoidal, corresponding to the original assumption of m. Although mathematically sound, this interpretation is physically invalid as the signal actually flows in a clockwise direction.

The reverse technique may not be applied to a nonlinearity possessing a zero slope over a non-finite input range, such as the ideal relay or saturation. The reverse characteristics of these nonlinearities possess infinite slope and hence have indeterminant equivalent sinusoidal gains.

The closed loop equations for the direct and reverse methods and the mathematical signal inversion will be more closely outlined in the following sections.

1.1.1 Closed Loop Equations

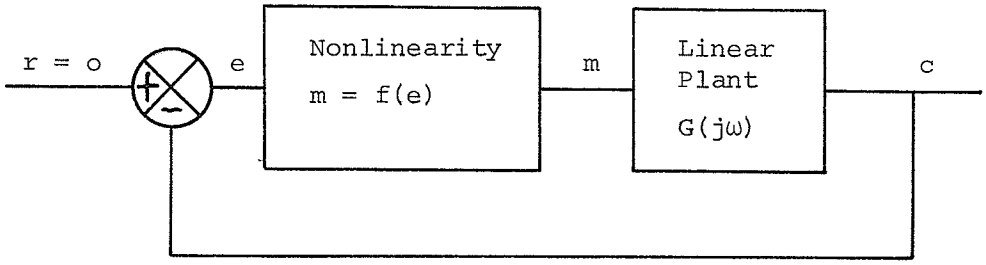

Fig. 1.2

CLOSED LOOP SYSTEM

The nonlinearity is defined by the relation $m=f(e)$. Applying the reverse technique, the reverse nonlinear characteristic is used and is defined by $e=f^{-1}(m)$ *.

*All nonlinearities except those excluded in Sec. 1.1 will have well defined inversions.

Direct Method - The input to the nonlinearity is assumed sinusoidal.

$$e \equiv E \sin \omega t \tag{1.1}$$

$$m = f(e)$$

$$= M \sin(\omega t + \alpha) + \text{higher harmonics} \tag{1.2}$$

α is the phase shift introduced by the nonlinearity. The equivalent direct sinusoidal gain of the nonlinearity is defined by:

$$Keq(E) \equiv \frac{M}{E} e^{j\alpha} \tag{1.3}$$

The closed loop equation is:

$$E = -M e^{j\alpha} G(j\omega)$$

$$= -Keq(E)\ E\ G(j\omega) \tag{1.4}$$

or
$$-1 = Keq(E)\ G(j\omega) \tag{1.5}$$

Reverse Method - The output of the nonlinearity is assumed sinusoidal.

$$m \equiv M \sin \omega t$$

$$e = f^{-1}(m) \tag{1.6}$$

$$= E \sin (\omega t + \beta) + \text{higher harmonics} \tag{1.7}$$

β is the phase shift introduced by the nonlinearity. The equivalent reverse sinusoidal gain of the nonlinearity is defined by:

$$Req(M) \equiv \frac{E}{M} e^{j\beta} \tag{1.8}$$

The closed loop equation is:

$$E\, e^{j\beta} = -M\, G(j\omega)$$

or $$M\, \mathrm{Req}\,(M) = -M\, G(j\omega) \qquad (1.9)$$

or $$\mathrm{Req}\,(M) = -G(j\omega) \qquad (1.10)$$

In both cases, the equivalent sinusoidal gains Keq(E) and Req(M) are the DF expressions for the nonlinear characteristics f(e) and $f^{-1}(m)$ respectively.

1.1.2 Path Inversion [2,3]

Signal-flow diagrams are a means of giving a detailed visual representation of the flow of signals through the system. Signal-flow theory may be used to justify the mathematical path inversion of the reverse method.

The standard closed loop system may be characterized by a flow graph of the following form:

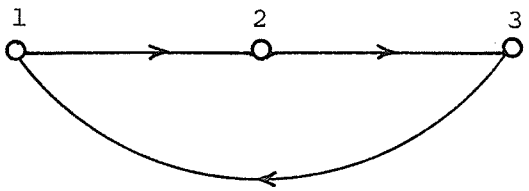

Fig. 1.3

SIGNAL-FLOW GRAPH, DIRECT CASE

Branch 12 contains the nonlinear element; branch 23 contains the linear plant; and branch 31 is the feedback path.

This flow graph typifies a system being analyzed in the usual forward direction. The gain in branch 23 is $G(j\omega)$.

If the linear plant is high pass, the reverse approach may be used. Mathematically speaking, the closed loop system may be analyzed in a counter-clockwise direction, beginning at the nonlinearity output. This means that the mathematical signal-flow path is from output to input of the linear plant. This requires signal inversion, which follows a general rule [3 p. 1153]: "The inversion of any branch jk is accomplished by reversing that branch and inverting its gain, and shifting any other branch ik having the same nose location k to the new position ij and dividing its gain by the negative of the original branch gain g_{jk}." Applying this rule, the signal-flow graph will now have the following form:

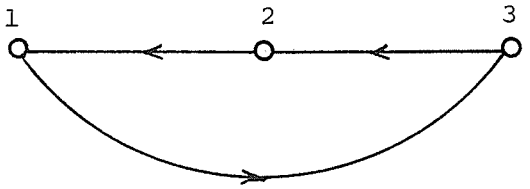

Fig. 1.4

SIGNAL-FLOW GRAPH, REVERSE CASE

The gain of branch 32 is now $\frac{1}{G(j\omega)}$. This essentially means that what was once a high pass system, in the forward direction, is now a low pass system in the reverse direction.

This is one of the major assumptions upon which the reverse approach is based; that the original high pass system becomes low pass in the reverse mode and filters out the higher harmonics produced by the nonlinearity.

Unfortunately, although the concept of the path inversion is theoretically ~~strong~~ sound, no clear physical interpretation exists. This reverse method appears to assume signal-flow in the opposite direction to that in the direct approach. In many cases this is physically impossible, as the model is in general, only valid for flow in one direction. Therefore, this mathematical interpretation may not be used to provide physical motivation for the reverse technique. Its use is mainly to give one a feeling for the reverse method, the idea that it may be appropriate in the high pass case.

1.1.3 Comments

This chapter has served to introduce the basic concepts of the reverse approach and has provided arguments to support its validity. The following chapters will provide an application of this method to specific problems, a definition of the boundary between the direct and reverse method, and certain low pass system applications.

CHAPTER 2

METHODS OF ANALYSIS

There are many methods of analysis which are readily applicable to nonlinear systems. Two computer oriented methods and a mathematical approach were chosen to solve for the nonlinear oscillations.

2.1 ANALOG COMPUTER

Analog computers are widely used as tools to study systems involving differential equations. The electronic analog computer uses computing elements which operate simultaneously, and whose outputs are voltages varying with time. System simulation was performed on an EAI 580 analog computer. The fundamental amplitude and frequency of the system oscillation can easily be determined, using Fourier analysis to determine the amplitude. Fourier analysis may be implemented in several different ways.

The most basic method is to multiply the system oscillation by a cosine and sine wave of the same fundamental frequency, and then integrate over one period. A switch is necessary to limit the integration to one cycle of oscillation. For accurate results, the multiplying sinusoid must have the same period as the system oscillation. Figure 2.1 gives a block diagram summary of this approach.

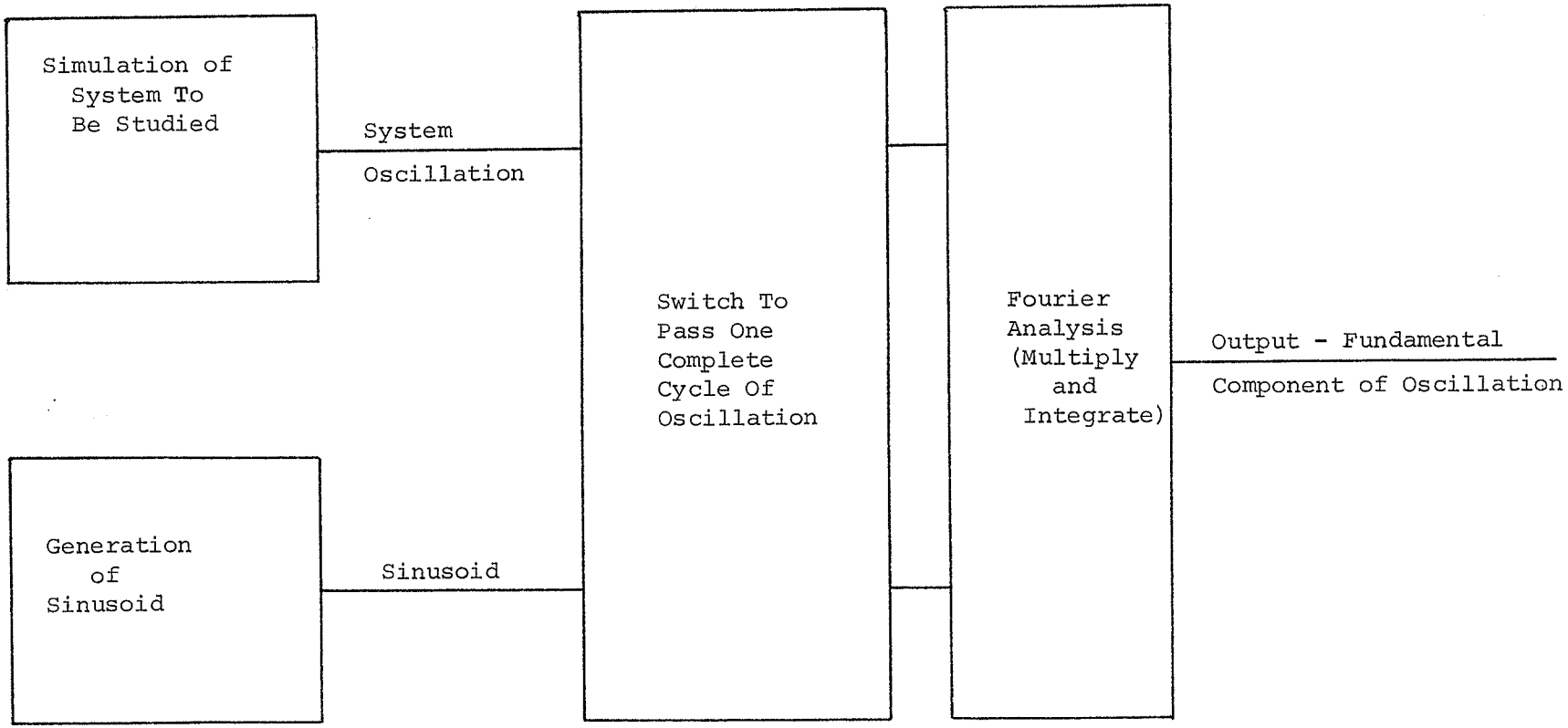

Fig. 2.1

BLOCK DIAGRAM OF ANALOG COMPUTER SIMULATION

An alternate method, proposed by Fifer [4], is more complicated mathematically but is physically simpler to realize. This method uses the response of an undamped harmonic oscillator which has been subjected to a forcing function (here the forcing function is the system oscillation). Again a switch is required to limit the analysis to one period of oscillation.

The latter method was chosen due to its high accuracy. This is possible as a result of the elimination of multipliers which are necessary to implement the first method. Multipliers on the analog computer are very inaccurate for low level inputs. A major disadvantage of the analog approach is that saturation considerations may demand a rescaling of the problem.

2.2 DIGITAL COMPUTER

The digital computer is especially suited to finding the solutions to the DF and the Dual Input Describing Function (DIDF) equations. A program available in the computer library, called Continuous System Modeling Program (CSMP), enables simulation of the nonlinear system. A discrete Fourier analysis program may then be applied to one cycle of the system oscillation to determine the amplitude of the fundamental and harmonic components after the steady state oscillation is achieved.

2.2.1 Numerical Techniques in General

The solution to the set of q equations

$$\begin{aligned} g_1\ (x_1,x_2,\ldots,x_p) &= 0 \\ g_2\ (x_1,x_2,\ldots,x_p) &= 0 \\ &\vdots \\ g_q\ (x_1,x_2,\ldots,x_p) &= 0 \end{aligned} \qquad (2.1)$$

is the set of p independent variables $(x_1,x_2,\ldots,x_p)$ which simultaneously satisfy the equations 2.1. If this set of independent variables is not a solution to 2.1, then not all the g_i will be zero, and

$$||g||^2 = g_1^2 + g_2^2 +\ldots+ g_q^2 \qquad (2.2)$$

will be a non-zero value. Most numerical techniques (including optimization methods) attempt to minimize such a norm or residual error. The major difficulty in multi-dimensional problems is that one cannot distinguish between the absolute minimum* and local minima.

In the simple two dimensional case, a local minimum is defined as follows [5]: "Suppose that f and its partial derivatives up to and including the third order are continuous near the point (a,b), and suppose that

$$f_x(a,b) = f_y(a,b) = 0$$

---

*Absolute minimum is the set of independent variables $(x_1,x_2,\ldots,x_p)$ which simultaneously satisfies 2.1 and makes $||g||^2 \equiv 0$.

Then (a,b) is a local minimum if

$$f_{xx}(a,b)\ f_{yy}(a,b) - f_{xy}^2(a,b) > 0$$

and $$f_{xx}(a,b) > 0 \quad ." \qquad (2.4)$$

Absolute and local minima both satisfy 2.3 and 2.4 and therefore are mathematically indistinguishable, except for the fact that the absolute minimum has a smaller norm.

Equations 2.3 and 2.4 may easily be extended to a multi-dimensional problem. The specific task here is to solve the DIDF equations, which consist of four equations in four unknowns, for the absolute minimum.

A solution algorithm or procedure suitable for execution on a digital computer must be constructed. Special attention must be paid to the various errors prevalent in this type of approach [6 pp.1-3].

Mathematical models of physical or natural processes inevitably contain some inherent errors. These errors result from incomplete understanding of natural phenomena, the stochastic or random nature of many processes, and uncertainties in experimental measurements. Often, a model includes only the most pertinent features of a physical process and is deliberately stripped of superfluous detail related to second-order effects. Algorithms that use only arithmetic operations and certain logic operations

such as algebraic comparison are called numerical methods. The error introduced in approximating the solution of a mathematical problem by a numerical method is usually termed the truncation error of the method. When a numerical method is actually run on a digital computer after transcription to computer program form, another kind of error, termed round-off error, is introduced. Round-off errors are caused by the rounding of results from individual arithmetic operations because only a finite number of digits can be retained after each operation, and will differ from computer to computer, even when the same numerical method is being used.

In light of these inescapable errors, one cannot expect to obtain precisely the absolute minimum by any known methods. Two optimization schemes were chosen to solve the DIDF problem at hand. One method is the Newton-Raphson iteration which found limited use because of the difficulty of finding the necessary partial derivatives. The other approach is a Pattern Search Optimization. This is a very time-consuming method even on a high speed digital computer, but is a suitable method when solving a nonlinear problem with many local minima. The Pattern Search will achieve a convex region independent of the shape of $||g||$. These methods will be discussed in the next two sections.

2.2.2 Pattern Search

The "Direct Search" solution of numerical and statistical problems was first introduced by R. Hooke and T.A. Jeeves [7]. This method was then applied to the problem of locating the minimum of a function by P.A. Macdonald [8]. The flow chart of Fig. 2.2 briefly outlines the procedural steps of this algorithm.

"Direct Search" describes sequential examination of trial solutions involving comparison of each trial solution with the "best" obtained up to that time together with a strategy for determining (as a function of earlier results) what the next trial solution will be. The application of direct search to a problem requires a space of points P which represent possible solutions, together with a means of saying that P_1 is a "better solution" than P_2 (written $P_1 \; C \; P_2$) for any two points in the space. There is presumably a single point P^*, the solution, with the property $P^* \; C \; P$ for all $P \neq P^*$. In these terms, the basic form of direct search is as follows. A point B_0 is arbitrarily selected to be the first "base point". A second point, P_1, is chosen and compared with B_0. If $P_1 \; C \; B_o$, P_1 becomes the second base point, B_1; if not, B_1 is the same as B_0. This process continues, each new point being compared with the current base point. The "strategy" for selecting new trial points is determined by a set of "states" which provide

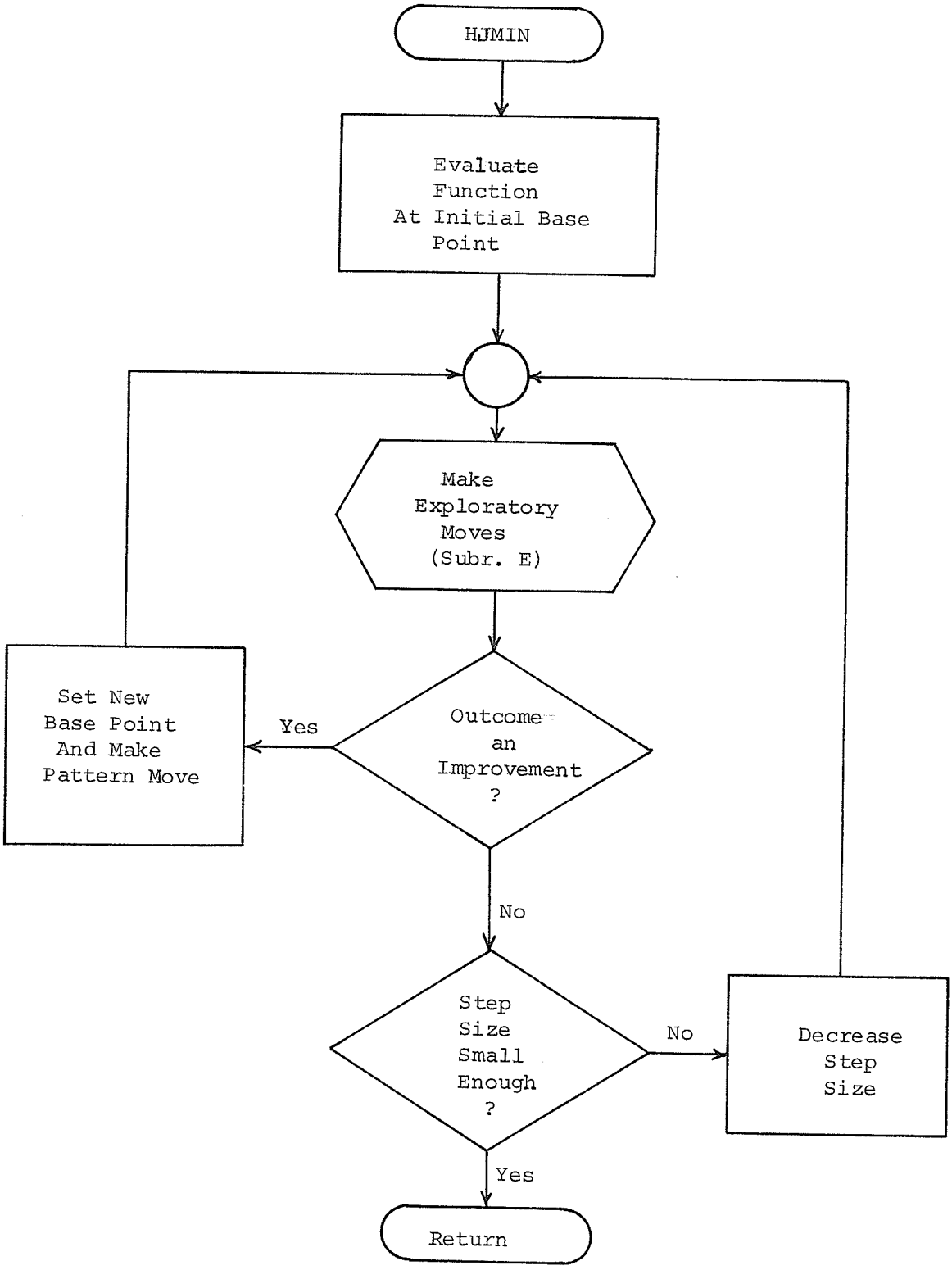

Fig. 2.2

FLOW CHART OF PATTERN SEARCH ALGORITHM

the memory. The number of states is finite. The kind of strategy used is dictated by various aspects of the problem, including one's knowledge of the structure of the solution space. The strategy itself comprises the choice of B_0 , the rules of transition between states, and the rules for selecting trial points as a function of current state and base point.

Pattern search, a specific kind of strategy, is a direct search routine for minimizing a function $S(\phi)$ of several variables $\phi = (\phi_1, \phi_2, \ldots, \phi_k)$. The argument ϕ is varied until the minimum of $S(\phi)$ is obtained. The pattern search routine determines the sequence of values for ϕ ; an independent routine computes the functional values of $S(\phi)$. This direct search procedure has been termed pattern search because it is based on the determination of a "pattern" of simple moves that will give a successful direction in which to move. The primary function of the exploratory moves is to supply information for the improvement of the pattern move.

The above optimization process has several drawbacks. A fairly accurate initial guess of the independent variables must be given. Starting at this point, the optimization routine does not guarantee an absolute minimum and may instead converge on a local minimum. The program attempts to minimize the norm of eqn. 2.2, but will never reach zero due to the inherent errors in the computer process.

This leaves the question, "At what point is the absolute minimum reached?" The "smallness" of the norm or residual which gives an acceptable result is a matter left to the discretion of the programmer. The process can be very time consuming if the function evaluations are complicated. Lastly, a problem may arise due to the different sensitivities of the g_i to small changes in the independent variables x_j. This may require the minimization of some normalized function instead of eqn. 2.2.

2.2.3 Newton-Raphson Iteration [6 pp.319-320, 9]

The Newton-Raphson method is a well known method for solving simultaneous nonlinear equations. This method is based on a simple principle which will be illustrated in one dimension.

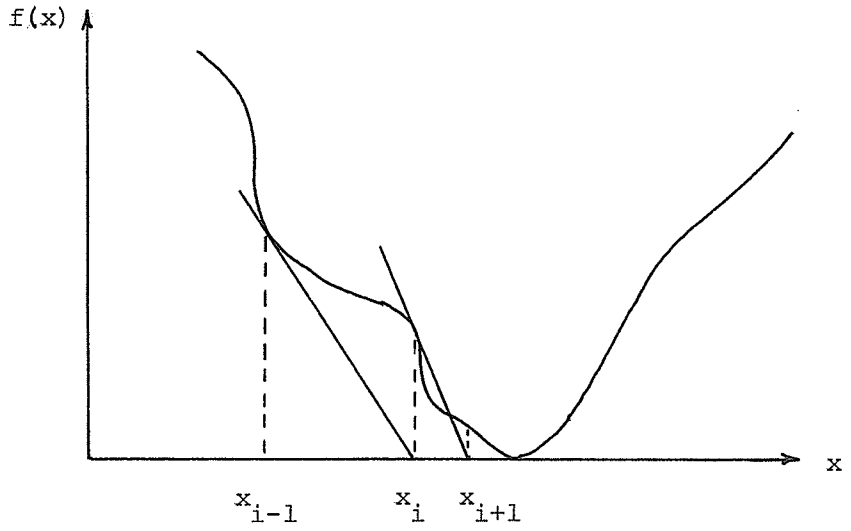

Fig. 2.3

I-D ILLUSTRATION OF NEWTON-RAPHSON METHOD

An initial guess is made at the point x_{i-1}. Through the point at $(x_{i-1}, f(x_{i-1}))$ a straight line is constructed which is tangent to $f(x)$ at $x=x_{i-1}$. The intersection of this line with the x-axis gives the next initial guess, x_i. This process is continued until the function has been reduced to a preset level. The speed of convergence depends entirely upon the initial guess, and a local minimum may be found instead of the absolute minimum.

The case at hand is a four dimensional problem, but is handled in basically the same manner. The set of equations

$$g_i(x_1, x_2, x_3, x_4) = 0 \quad , \quad i=1,2,3,4 \tag{2.5}$$

may be written in the form

$$\underline{g}(\underline{x}) = \underline{0} \tag{2.6}$$

where $\underline{x}$ is a ~~row~~ column vector of the four independent variables. If $\underline{x}_i$ is the i^{th} approximation to the solution of 2.5, then the next approximation $\underline{x}_{i+1}$ is given by

$$\underline{x}_{i+1} = \underline{x}_i - A_i^{-1} \, \underline{g}(\underline{x}_i) \tag{2.7}$$

where A_i is the matrix $(g_{ij}(\underline{x}_i))$, $i=1,2,3,4$ and $j=1,2,3,4$

where $$g_{ij}(\underline{x}_i) = \frac{\partial g_i(\underline{x}_i)}{\partial x_j} \tag{2.8}$$

The major disadvantage of this method is that the

first order partial derivatives of g_i are required and they can be easily found only if the nonlinearity is a single-valued, differentiable curve.

2.2.4 Continuous System Modeling Program

The S/360 CSMP is a problem-oriented program designed to facilitate the digital simulation of continuous processes on large-scale digital machines. The program provides an application-oriented language that allows these problems to be prepared directly and simply from either a block-diagram representation or a set of ordinary differential equations. The program includes a basic set of functional blocks with which the components of a continuous system may be represented, and accepts application-oriented statements for defining the connections between these functional blocks. The self-oscillation of time invariant, nonlinear problems may readily be observed using this program.

2.3 EXACT METHODS

The exact method is a mathematical solution of the closed loop equation, and involves no approximations or error. It is applicable only to the simplest examples, as more complex systems result in formidable calculations. It is for this reason that the exact method was seldom considered as a reasonable approach.

CHAPTER 3

THE DF AND ITS CALCULATION

Throughout the history of control studies, linear theory has become the most advanced and simplified form of analysis. It is not surprising that, due to the analytic difficulty of nonlinear problems, an attempt has been made to approximate the nonlinearity so that linear theory may be applied. The remodeling must preserve the nonlinear property of interest. One attempt to apply linear theory to nonlinear problems has led to the Describing Function (DF).

The DF method developed through the harmonic linearization method of Krylov and Bogoliubov [1 p.46] and can be attributed to a large number of authors. The DF is an approximate technique used to study the existence, form, and stability of oscillations in autonomous, nonlinear systems. Inherent in this method is an approximation of the shape of the oscillation waveform. Then, the conditions under which this form of oscillation will exist, approximately, in the system must be found.

3.1 FORMULATION OF THE DF

Consider the single nonlinearity, closed loop system of Fig. 3.1; in general the nonlinear element will be one of:

(a) Static, single-valued

(b) Multivalued (hysteretic)

(c) Dynamic

This thesis will be restricted to the static, single-valued case. There are three basic conditions involved in the DF [1 p.110]:

(a) The nonlinear element is time invariant.

(b) No subharmonics are ~~generated by the nonlinearity in response to a sinusoidal input~~ present in the system.

(c) The linear element acts as a low pass filter and attenuates the harmonics of $m(t)$. This is known as the filter hypothesis.

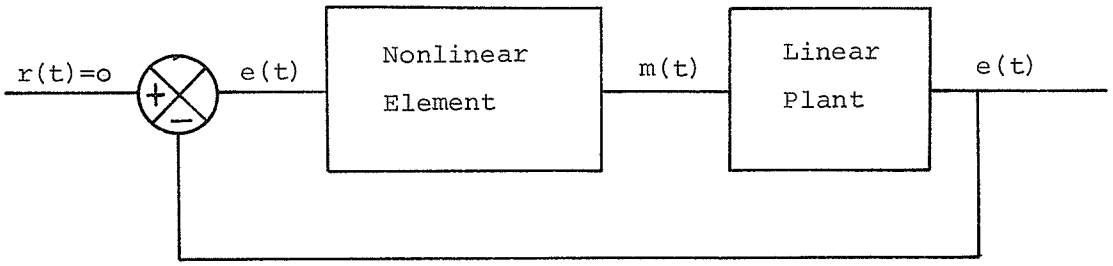

Fig. 3.1

GENERAL AUTONOMOUS, NONLINEAR SYSTEM

The DF method involves finding the describing function for the nonlinear element, which is its equivalent gain to a sinusoidal input $E \sin \omega t$. The ordinary DF for a general nonlinearity, $m=f(e,\dot{e})$, is the complex quantity

$$K_{eq}(E,\omega) = g(E,\omega) + j\, b(E,\omega) \qquad (3.1)$$

where

$$g(E,\omega) \equiv \frac{1}{\pi E}\int_0^{2\pi} f(E \sin u, E\,\omega \cos u)\, \sin u\, du \qquad (3.2)$$

and

$$b(E,\omega) \equiv \frac{1}{\pi E}\int_0^{2\pi} f(E \sin u, E\,\omega \cos u)\, \cos u\, du \qquad (3.3)$$

In general, the DF depends upon both amplitude (E) and frequency (ω), and is complex. In the case of the static, single-valued nonlinearity, $m=f(e)$, the DF is real and frequency independent:

$$K_{eq}(E,\omega) = K'_{eq}(E) = g(E) = \frac{1}{\pi E}\int_0^{2\pi} f(E \sin u)\, \sin u\, du \qquad (3.4)$$

where

$$b(E) = \frac{1}{\pi E}\int_0^{2\pi} f(E \sin u)\, \cos u\, du \equiv 0 \qquad (3.5)$$

If the nonlinearity is static but multivalued, then it cannot be expressed as a single-valued $f(e)$ or even $f(e,\dot{e})$, but the DF can still be computed. In this case,

$$K'_{eq}(E) = g(E) + j\, b(E) \qquad (3.6)$$

is, in general, complex and frequency independent, with

$$g(E) \equiv \frac{1}{\pi E}\int_0^{2\pi} f(E \sin u)\, \sin u\, du \qquad (3.7)$$

and $$b(E) \equiv \frac{1}{\pi E}\int_0^{2\pi} f(E \sin u)\, \cos u\, du \qquad (3.8)$$

←——— It must be remembered that the present value of $f(E \sin u)$ is dependent on the past history of $f(E \sin u)$.

The linearized, closed loop system of Fig. 3.1 now has the form of Fig. 3.2.

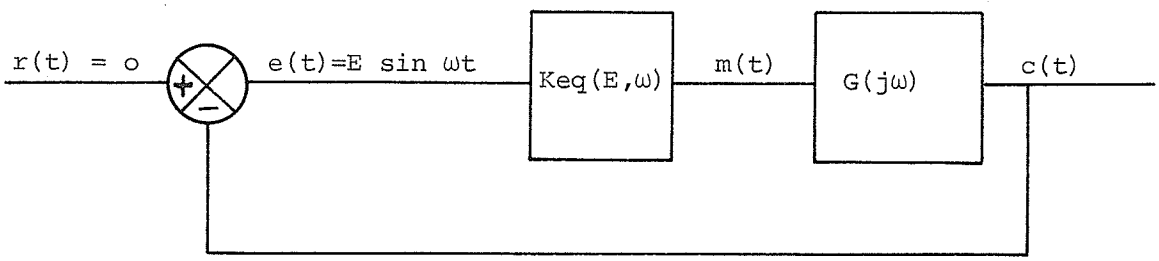

Fig. 3.2

LINEARIZED, CLOSED LOOP SYSTEM FOR CONVENTIONAL DF

3.2 FORMULATION OF THE rms DF [1 p.85, 10]

Various unconventional describing functions have been proposed but these have not found widespread use as they require more work and do not, in general, consistently provide the accuracy of the conventional DF. It is apparent that as the linear element of the closed loop tends toward a perfect low pass filter, the error of the conventional DF and some unconventional DF's tends toward zero. It is possible, however, that an unconventional DF could provide better accuracy for many practical systems since perfect filtering is unrealistic.

In 1961, J.E. Gibson and K.S. Prasanna-Kumar [12] proposed the Root Mean Square describing function (rms DF) for single-valued, instantaneous nonlinearities. This may be applied to the system in Fig. 3.1. The rms DF is obtained by equating the rms value of the equivalent output sine wave of fundamental frequency to the rms value of the

nonsinusoidal output of the nonlinear element in response to a sine-wave input. This might be justified on an equivalent energy basis. The definition is

$$\text{rms DF} = \text{RMSeq}(E)^{*} = \left\{ \frac{\frac{1}{2\pi}\int_0^{2\pi}\left[f(E \sin u)\right]^2 \, du}{\frac{1}{2\pi}\int_0^{2\pi}(E \sin u)^2 \, du} \right\}^{\frac{1}{2}} \qquad (3.9)$$

where $E \sin u$ is the input to the nonlinearity and $f(E \sin u)$ is the output of the nonlinearity.

For instantaneous nonlinearities, the phase shift through the element will be zero. The linearized, closed loop system is shown in Fig. 3.3.

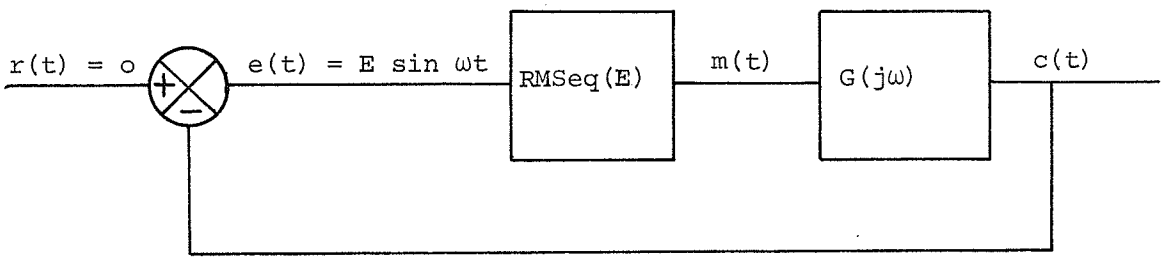

Fig. 3.3

LINEARIZED, CLOSED LOOP SYSTEM FOR rms DF

3.3 APPLICATION TO SYSTEM ANALYSIS

The remaining sections of this chapter will deal with the equivalent gain obtained by the conventional DF.

*RMSeq(E) - Equivalent gain of the nonlinear element using the rms describing function.

Should the rms DF be used, a simple substitution of equivalent gains is all that is required to analyze the problem.

The DF-predicted oscillation may now be found using the linearized model of Fig. 3.2. The calculations are greatly simplified due to the constant coefficients involved for each E and ω. The DF method is simply to constrain the loop gain to a sinusoidal signal to 1 or

$$Keq(E,\omega)\ G(j\omega) = -1 \tag{3.10}$$

The common approach is to write eqn. 3.10 as

$$G(j\omega) = \frac{-1}{Keq(E,\omega)} \tag{3.11}$$

and then solve graphically. The linear ~~plant~~ t.f., $G(j\omega)$, is plotted in polar form as a function of frequency ω, as in the standard Nyquist diagram. The "critical locus" $\frac{-1}{Keq(E,\omega)}$, for each of a set of values of ω, is plotted on the same graph, as a function of amplitude E. The intersection of $G(j\omega)$ and $\frac{-1}{Keq(E,\omega)}$, for which the ω values match normally corresponds to an oscillation. If the DF is frequency independent, the intersection of $G(j\omega)$ and $\frac{-1}{K'eq(E)}$ will lead to oscillation.

If the single-valued nonlinearity is odd and symmetric, $f(e)=-f(-e)$, the resulting oscillation will usually involve only the odd harmonics, and no dc bias.

3.4 STABILITY OF OSCILLATION

The question of limit cycle stability is posed in terms of the behaviour of a theoretical limit cycle state following amplitude and/or frequency perturbations. If the limit cycle returns to its original equilibrium state, it is called stable, whereas if either its amplitude or frequency grows or decays, it is called unstable. There are a few general approaches to the stability question; Loeb's criterion, the Incremental-Input Describing Function (IDF) technique, and a graphical approach.

3.4.1 Loeb's Criterion [1 pp.121-123]

This stability approach is based on the assumption of a certain specific form of perturbation about the DF predicted oscillation. The predicted oscillation $E_o e^{j\omega_o t}$ is perturbed in amplitude by ΔE and in frequency by $\Delta\omega + j\Delta\tau$, where $\Delta\tau$ represents damping. A concise derivation of the criterion may be found in Gille et al. [12]. This approach results in the evaluation of the following cross product to determine stability for frequency independent nonlinearities.

$$\frac{\partial\, \underline{G}(j\omega)}{\partial\omega} \times \frac{\partial\, \frac{-1}{\underline{K}'eq(E)}}{\partial E} \qquad (3.12)$$

The oscillation at a specific amplitude and frequency (E_o, ω_o) will be stable if the resultant vector in

eqn. 3.12, evaluated at (E_o, ω_o) , points out of the page. Similarly, the oscillation will be unstable if the resultant vector points into the page. A basic example of this criterion is shown in Fig. 3.4.

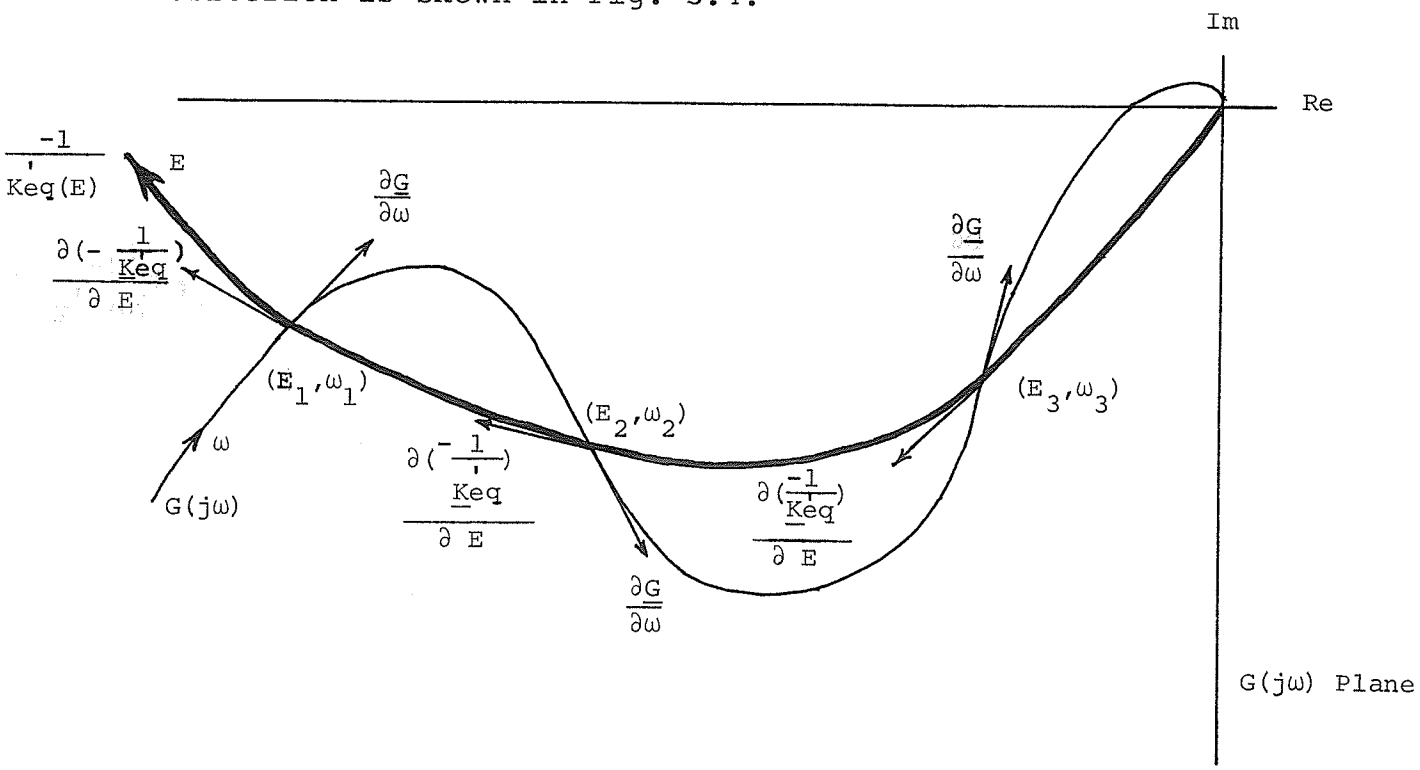

Fig. 3.4

EXAMPLE OF LOEB'S CRITERION FOR STABILITY OF OSCILLATION

From Fig. 3.4, intersections (E_1, ω_1) and (E_3, ω_3) would result in stable limit cycles, while an oscillation at (E_2, ω_2) would be unstable.

3.4.2 IDF Stability Technique [13]

The Incremental-Input Describing Function (IDF) stability technique is based on the calculation of the equivalent gain of the nonlinearity to an infinitesimal

signal in the presence of the DF predicted sinusoidal oscillation. This infinitesimal signal may be, for example, a bias or a sinusoid. A technique for calculating the IDF may be found in Gelb et al. [1 pp.276-278]. The linearized IDF system is a constant coefficient system and any linear system stability technique (Nyquist, Routh-Hurwitz, root locus) may be applied to it to determine stability.

3.4.3 Graphical Technique

The graphical argument comes from linear system theory, which states: "If the limit cycle amplitude perturbation is positive, a stable system configuration is required to dissipate energy until the amplitude decays to its unperturbed value; if the amplitude perturbation is negative, an unstable system configuration is required to absorb energy until the amplitude grows to its unperturbed value." This approximates local stability. An example of this approach is shown in Fig. 3.5.

The shaded areas represent the stable regions. If the system is at 3, a negative perturbation will drive the system into an unstable region. This will cause the system amplitude to grow until state 3 is reached again. A small positive perturbation from 3 will drive the system into a stable region, where the system amplitude will decrease until state 3 is again reached. A similar investigation of states 1 and 2 will show that states 1 and 3 are stable,

while 2 is unstable.

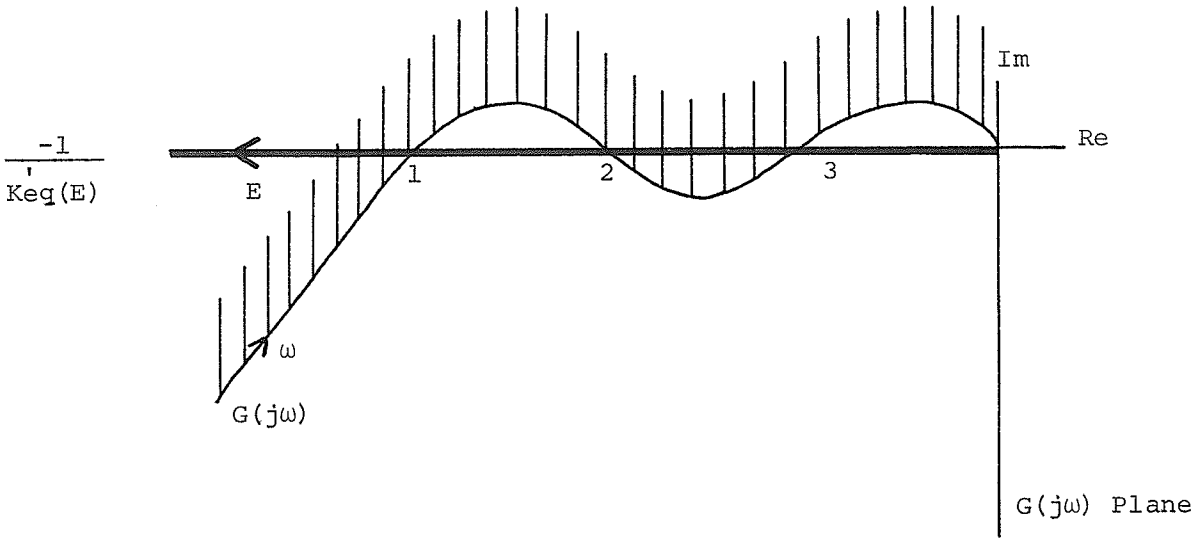

Fig. 3.5

EXAMPLE OF GRAPHICAL STABILITY TECHNIQUE

3.5 ACCURACY OF THE DF APPROXIMATION

The value of any approximate method of analysis is limited by the confidence the designer has in the results. In one case, a 1% deviation from the actual value may be acceptable, while in another, a 0.1% or a 10% deviation may be justified. Because no known standards are available, a heavy reliance must be placed on logical and intuitive evaluation. The validity of the DF method is primarily based on intuition and experimental results.

The objective of this thesis is to show that the reverse approach in particular examples is more accurate than the direct approach. There are many different ways of assessing the degree of accuracy and several will be outlined

in this section. This question of accuracy pertains only to amplitude as both methods predict the same fundamental frequency of oscillation.

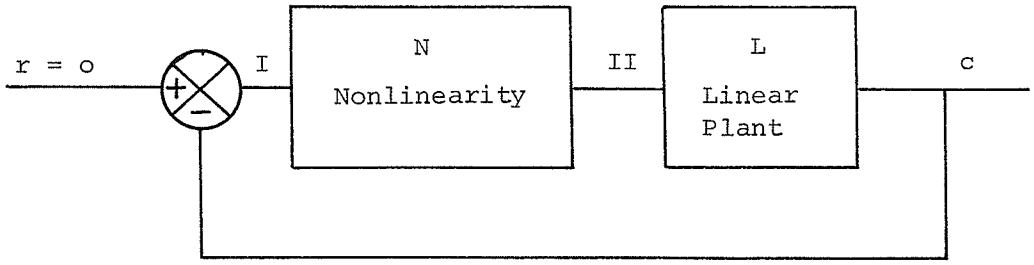

Fig. 3.6

GENERAL FORM OF FEEDBACK SYSTEM, THE DIRECT METHOD ASSUMES A SINUSOID AT I, WHILE THE REVERSE METHOD ASSUMES A SINUSOID AT II.

The closed loop equations derived in Sec. 1.1.1 are used to find the magnitudes of the fundamental components at I and II by the direct and reverse DF methods respectively. These fundamental magnitudes may then be transferred from the input to the output of the nonlinearity, or vice-versa, through the linear plant. Simulation techniques are used to find the actual waveforms, and hence the actual fundamental magnitudes at I and II. One of the following methods may be used to assess the "goodness" of the DF approximation.

Method I: Theory and actual are compared at the nonlinearity input. The two theoretical values are the magnitudes of the fundamental component at I (direct DF) and the

fundamental component at II (reverse DF) transferred to I. The measure of error is defined as the percentage difference between each theoretical value and the actual magnitude of the fundamental component at I. The better approximation (direct or reverse) is determined by which gives the lesser percentage error.

Method II: Theory and actual are compared at the nonlinearity output. The two theoretical values are the magnitudes of the fundamental component at II (reverse DF) and the fundamental component at I (direct DF) transferred to II. The measure of error is defined as the percentage difference between each theoretical value and the actual magnitude of the fundamental component at II. The better approximation (direct or reverse) is determined by which gives the lesser percentage error.

Method III: Theory and actual are compared at both the nonlinearity input and output. The direct DF approximation at I and the actual fundamental magnitude at I are compared to give a percentage error. The reverse DF approximation at II and the actual fundamental magnitude at II are compared to give another percentage error. The lesser percentage error determines which approximation (direct or reverse) is better.

Method IV: This method is an assessment of the harmonic imbalance in the loop. In the direct case, the loop is traversed in a clockwise direction from I. Considering

the return signal to I, the magnitude of the most significant harmonic (usually the third) is compared with the magnitude of the fundamental component. In the reverse case, the loop is traversed in a counter-clockwise direction from II. Considering the return signal to II, the magnitude of the most significant harmonic is compared with the magnitude of the fundamental. The better approximation (direct or reverse) is determined by which gives the lesser harmonic imbalance.

The whole principle of the DF method involves an assumed waveform at some point in the system loop. It seems only logical that the accuracy of this assumption can be best assessed by determining the actual waveform at this same point. Otherwise, if the comparison is made at some other point in the circuit, the assumption must be transferred through system blocks, and this may introduce error due to slight frequency differences (and hence a change in linear gain) between theory and actual.

Methods I and II involve amplitude translations of the reverse and direct approximations respectively, and therefore are inaccurate. Method III is far better, as the actual and assumed waveforms are evaluated at the same point, in each of the direct and reverse cases. This is the method that will be used in the examples of Chapters 4 and 7.

The fourth method gives an estimate of the harmonic content that is ignored in the approximation. The decision

of direct or reverse being more accurate does not require knowledge of the actual waveform at I or II, and hence greatly simplifies matters. This criterion may possibly find use in determining, before simulation, which of the direct or reverse methods will be more accurate. This idea has not been thoroughly investigated, as this would require the solution of many example problems in order to observe general trends.

In spite of the above arguments, each method warrants special attention and the decision on which to adopt is ultimately up to the user and his discretion.

CHAPTER 4

APPLICATION OF THE REVERSE DF AND REVERSE rms DF

The methods developed in the previous chapters will now be applied to specific examples. Each system is made up of a static, single-valued nonlinearity and a high pass linear plant. In each case, the reverse DF and reverse rms DF techniques will be compared with the direct DF and direct rms DF.

4.1 EXAMPLE 1

The system is made up of a gain-changing nonlinearity and the linear plant $\frac{K\,S(S+.5)(S+1)}{(S+8)(S+10)(S+15)^2}$.

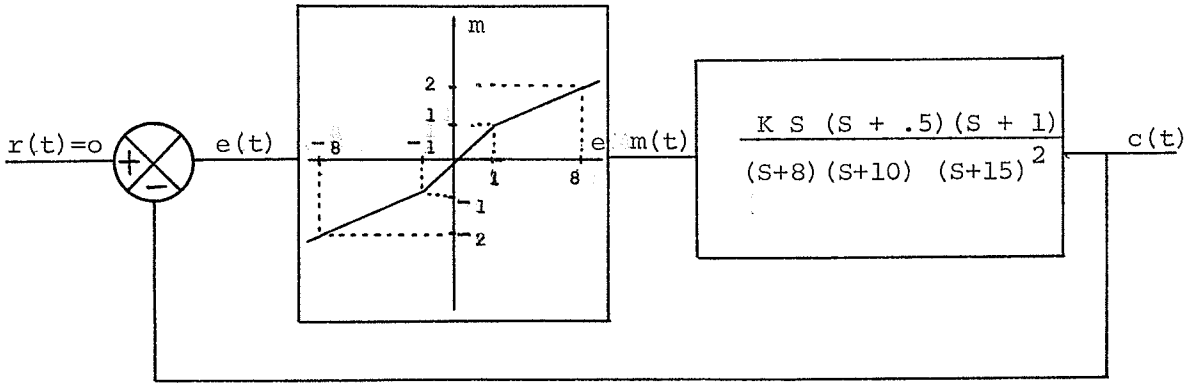

Fig. 4.1

CLOSED LOOP SYSTEM OF EXAMPLE 1

As evident from Fig. 4.2, this system has two possible oscillatory states. The state at ω = 3.212 rad./sec. exhibits a stable oscillation, while the state at ω = 1.07

rad./sec. is an unstable mode. Operating at $\omega = 3.212$ rad./sec., the linear plant possesses high pass characteristics in a sufficient range to include significant harmonics; this is indicated by the Bode diagram of Fig. 4.3.

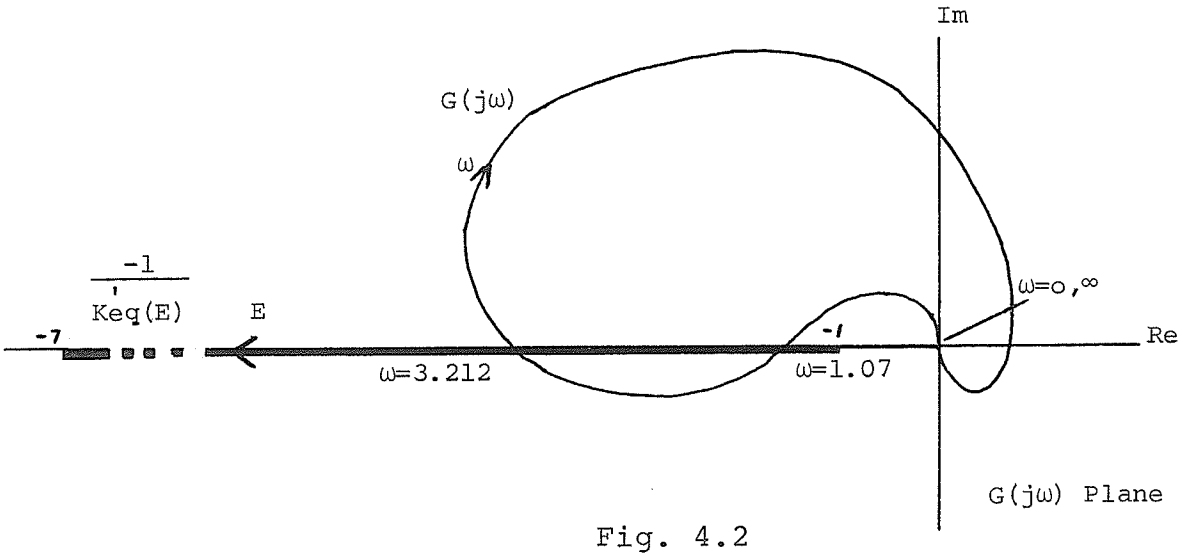

Fig. 4.2

FREQUENCY AND AMPLITUDE LOCI, EXAMPLE 1

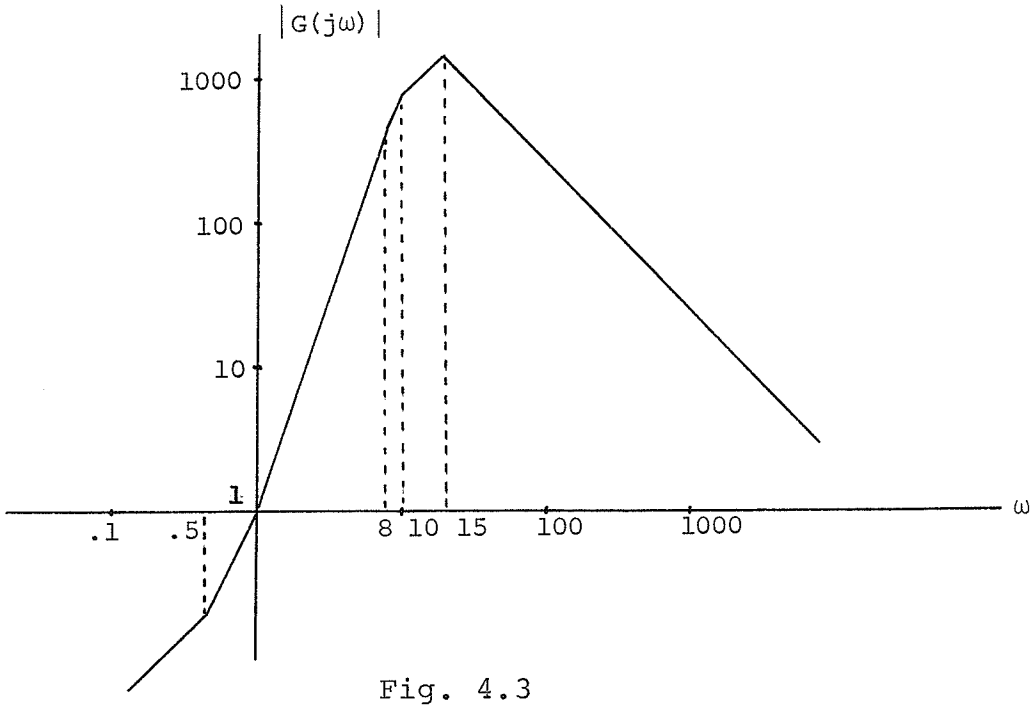

Fig. 4.3

BODE DIAGRAM OF HIGH PASS SYSTEM, EXAMPLE 1

The direct DF and direct rms DF methods are used to determine the fundamental amplitudes for various values of gain K, by assuming $e(t)=E \sin \omega t$. Then, assuming $m(t)=M \sin \omega t$, the reverse technique is used to determine again the fundamental magnitudes for various K values. Simulation on the digital computer provided the actual fundamental components of e(t) and m(t) .

TABLE 1

DIRECT DF AND REVERSE DF, DIGITAL SIMULATION, EXAMPLE 1

K	E_D*	Measured E	% Error in E**	M_R***	Measured M	% Error in M**
660	1.230	1.139	8.02	1.056	1.053	0.23
900	1.962	1.640	19.66	1.202	1.159	3.69
1125	2.688	2.177	16.97	1.329	1.280	3.92
1800	5.592	4.614	21.19	1.792	1.671	7.14
2250	8.592	7.321	17.36	2.242	2.083	7.61
2850	15.580	14.098	10.51	3.266	3.075	6.20
3375	29.450	27.761	6.09	5.288	5.043	4.86
3750	57.730	57.539	0.33	9.322	9.306	0.17

*E_D - Predicted fundamental amplitude of e(t) using the direct method.

**% ERROR - This is the error explained in Method III, Sec. 3.5.

***M_R - Predicted fundamental amplitude of m(t) using the reverse method.

TABLE 2

DIRECT rms DF AND REVERSE rms DF, DIGITAL COMPUTER, EXAMPLE 1

K	E_D	Measured E	% Error in E	M_R	Measured M	% Error in M
660	1.233	1.139	8.29	1.053	1.053	0.008
900	2.006	1.640	22.35	1.186	1.159	2.300
1125	2.776	2.177	27.51	1.301	1.280	1.650
1800	5.869	4.614	27.21	1.734	1.671	3.770
2250	9.022	7.321	23.23	2.172	2.083	4.250
2850	16.148	14.098	14.54	3.177	3.075	3.310
3375	30.310	27.761	9.18	5.181	5.043	2.740
3750	58.585	57.539	1.82	9.221	9.306	0.910

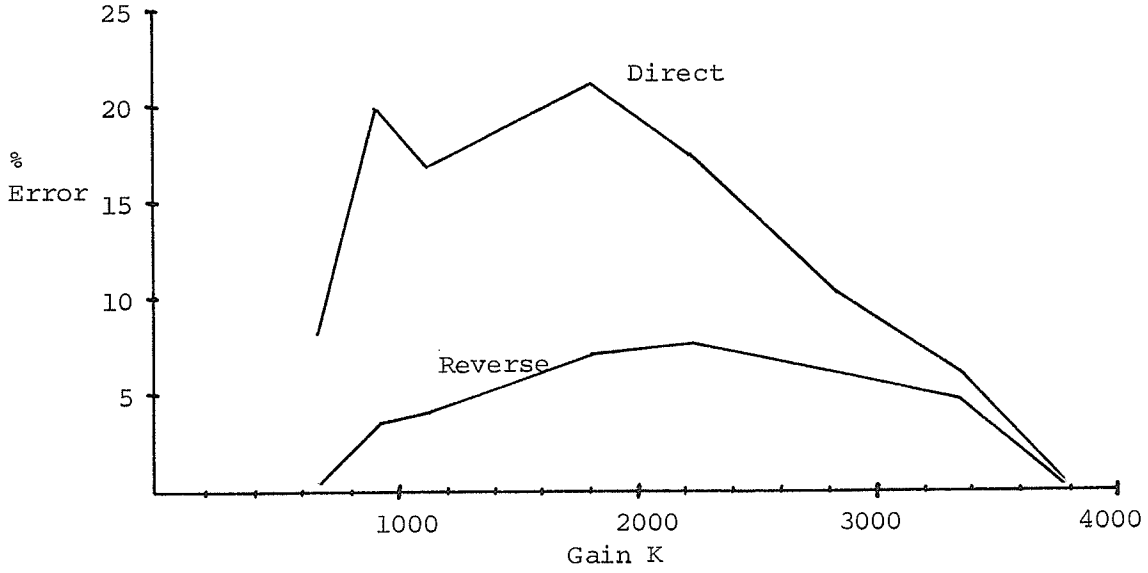

Fig. 4.4

ERRORS IN THE DIRECT AND REVERSE DF METHODS, EXAMPLE 1

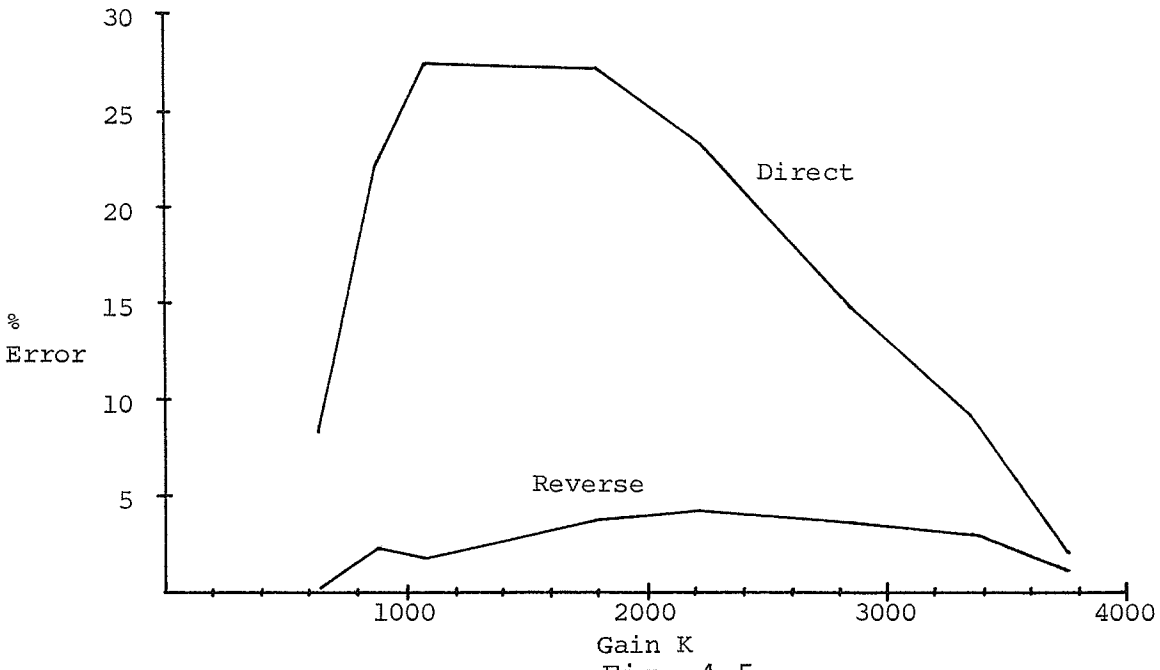

Fig. 4.5

ERRORS IN THE DIRECT AND REVERSE rms DF METHODS, EXAMPLE 1

The digital simulation exhibits a fundamental frequency of 3.092 rad./sec. for all the various K values, which is 3.74% below the theoretical frequency. The oscillation amplitude increases as a function of system gain. For large values of gain, the break points of the nonlinearity at ±1 become insignificant and the characteristic becomes almost linear. As a result, the harmonic content of the nonlinearity output (and hence input) drops, and the direct and reverse methods both become very accurate. Similar linearization occurs for oscillation amplitudes only slightly larger than 1.0.

The tabulated results indicate that the direct DF and direct rms DF give very large errors for a wide range of values of K . This may be attributed to the high pass linear plant, which does not attenuate the higher harmonics

produced by the nonlinearity. The harmonic content of the input to the nonlinearity varies with the gain K , having a maximum third harmonic to fundamental ratio of 23% at K = 1800. The largest error in E also occurs at K = 1800, which indicates a correlation between harmonic content and error. The less sinusoidal the signal becomes at the nonlinearity input, the higher is the resulting error in the DF approximation. Because of the relatively large errors involved, the sinusoidal assumption at the nonlinearity input (direct method) is very crude.

In comparison, the reverse DF and reverse rms DF results are very good, deviating from the actual by less than 7.61%. The harmonic content at the nonlinearity output again varies with K , but only reaches a maximum third harmonic to fundamental ratio of 3.46%. The sinusoidal assumption at m(t) (reverse method) is therefore justified. The reverse rms DF offers a slight improvement over the reverse DF.

4.2 EXAMPLE 2

This example studies the autonomous system made up of a cube root nonlinearity $m = e^{1/3}$ and the linear plant $\frac{K S^3}{(S+2)^3(S+50)}$.

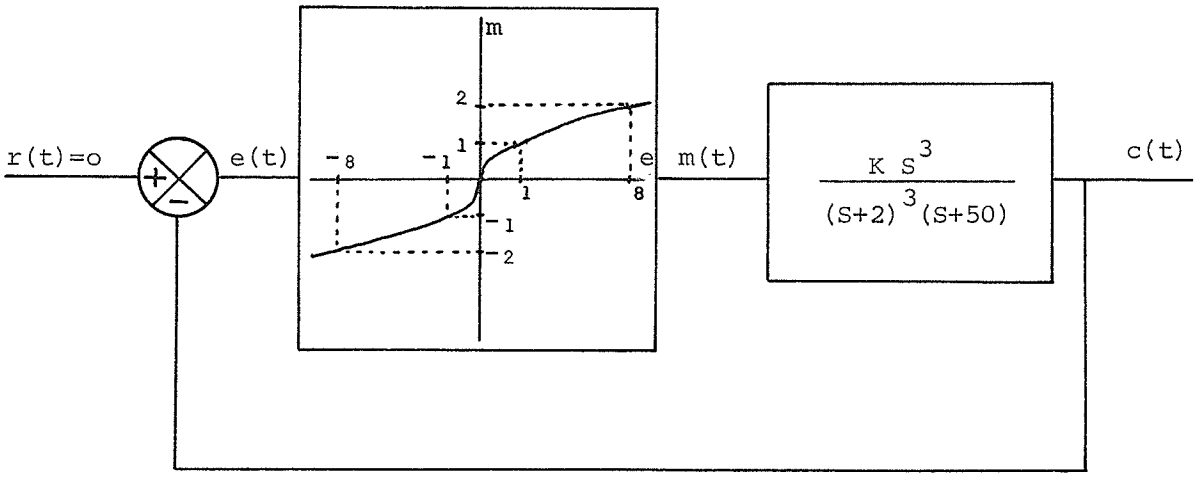

Fig. 4.6

CLOSED LOOP SYSTEM OF EXAMPLE 2

The system possesses one possible limit cycle state at ω = 1.13462 rad./sec., which is stable. The amplitude and frequency loci of this system are shown in Fig. 4.7, while Fig. 4.8 gives the frequency response of the linear plant. As in Example 1, the direct and reverse DF and rms DF methods were used to calculate the fundamental oscillation amplitudes at the input and output to the nonlinearity. The actual amplitudes of oscillation were found by simulation on the digital computer.

From digital simulation, the fundamental frequency of oscillation was found to be 1.074 rad./sec., which was 5.33% below the predicted value. Varying the gain K did not change the frequency of oscillation, but directly influenced the amplitude of oscillation.

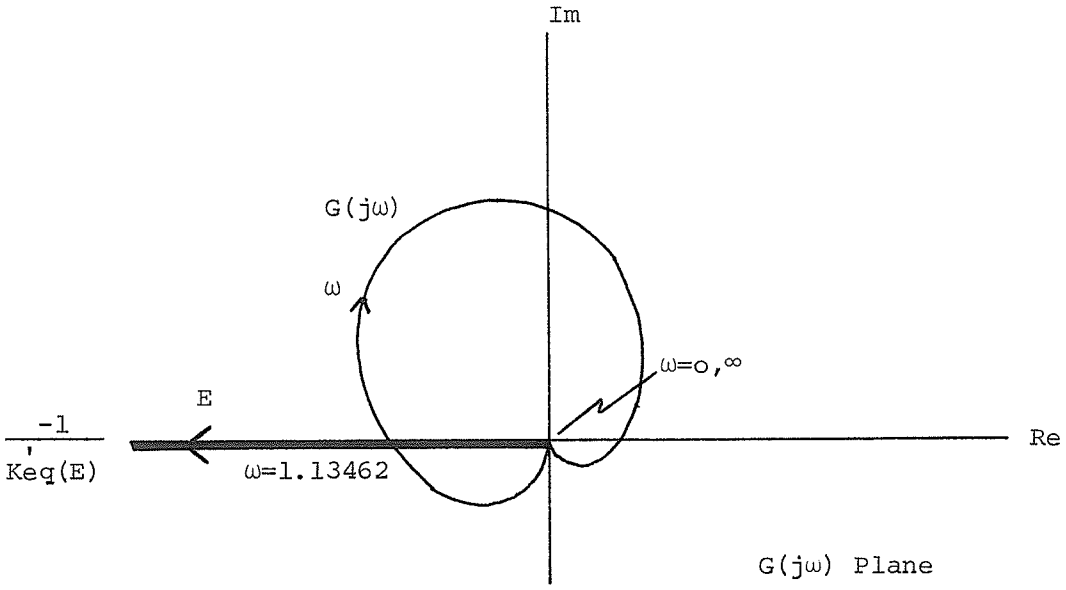

Fig. 4.7

FREQUENCY AND AMPLITUDE LOCI, EXAMPLE 2

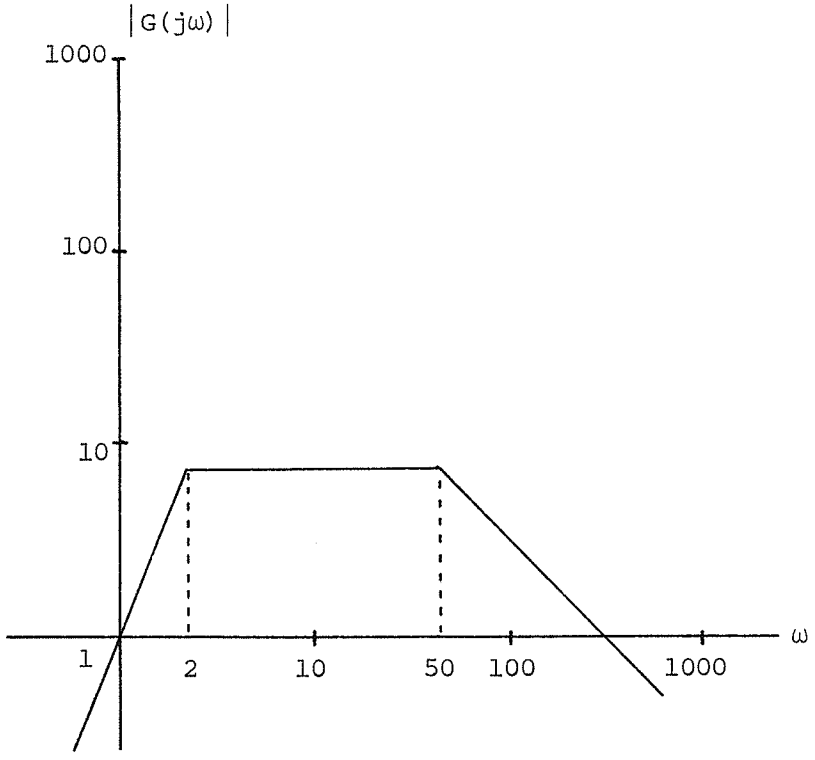

Fig. 4.8

BODE DIAGRAM OF HIGH PASS SYSTEM, EXAMPLE 2

TABLE 3

DIRECT DF AND REVERSE DF, DIGITAL SIMULATION, EXAMPLE 2

K	E_D	Measured E	% Error in E	M_R	Measured M	% Error in M
100	0.1471	0.119	24.08	0.5659	0.541	4.69
300	0.7643	0.613	24.64	0.9802	0.953	2.85
600	2.1619	1.758	22.98	1.3863	1.338	3.65
1250	6.5008	5.251	23.81	2.0009	1.946	2.82
2200	15.1788	12.210	24.31	2.6545	2.541	4.47
3000	24.1705	19.420	24.46	3.0998	2.979	4.07
4000	37.2129	29.868	24.59	3.5794	3.427	4.44

TABLE 4

DIRECT rms DF AND REVERSE rms DF, DIGITAL SIMULATION, EXAMPLE 2

K	E_D	Measured E	% Error in E	M_R	Measured M	% Error in M
100	0.154	0.119	30.03	0.551	0.541	1.96
300	0.801	0.613	30.56	0.955	0.953	0.19
600	2.265	1.758	28.85	1.350	1.338	0.97
1250	6.800	5.251	29.54	1.949	1.946	0.15
2200	15.913	12.210	30.22	2.586	2.541	1.76
3000	25.320	19.420	30.38	3.019	2.979	1.36
4000	38.980	29.868	30.50	3.486	3.427	1.73

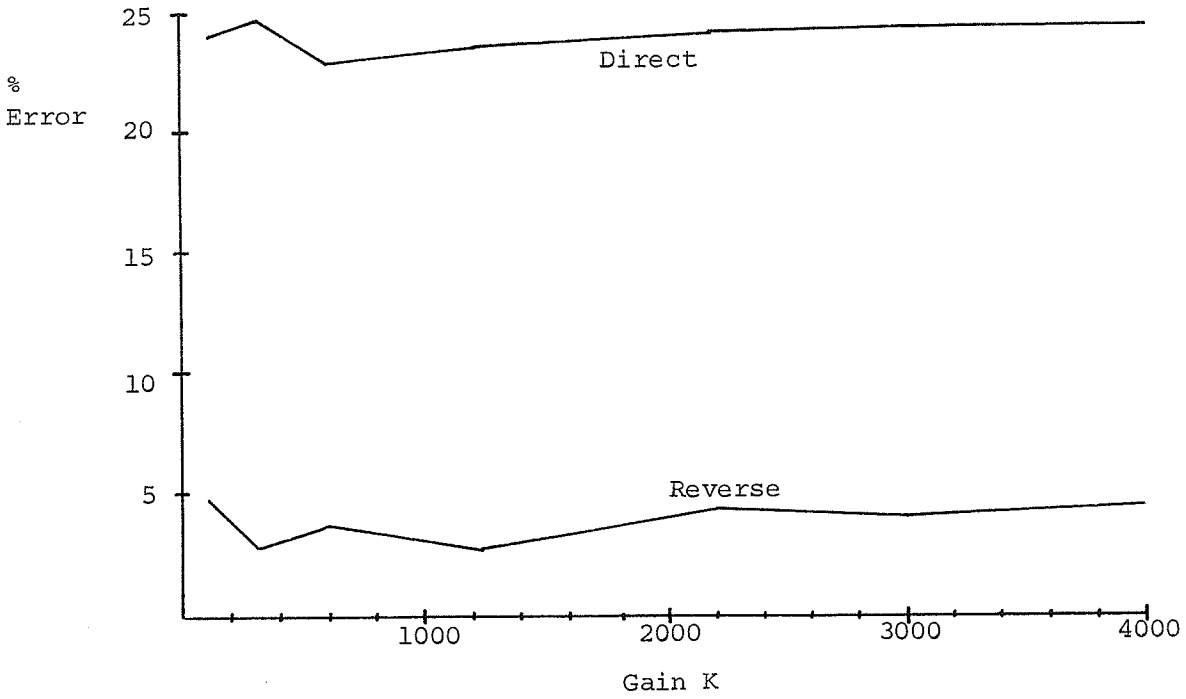

Fig. 4.9

ERRORS IN THE DIRECT AND REVERSE DF METHODS, EXAMPLE 2

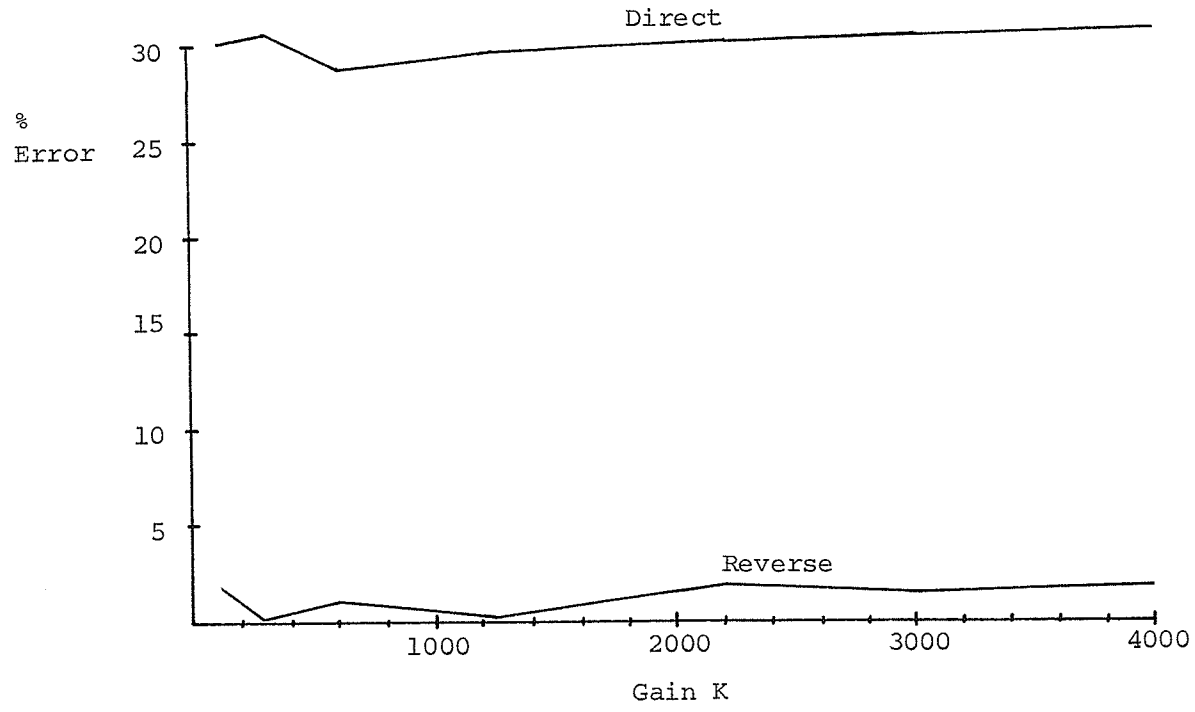

Fig. 4.10

ERRORS IN THE DIRECT AND REVERSE rms DF METHODS, EXAMPLE 2

The direct methods give very poor results, the smallest error from the actual being 24%. These large errors result from the high ratio of third harmonic to fundamental at the nonlinearity input, which ranges from 27% to 31% for various values of gain K. The assumption of a sinusoid at the input to the nonlinearity is very inaccurate.

In contrast, the reverse techniques yield very accurate results. The error in the reverse DF case was less than 4.69%, while the error in the reverse rms DF case was less than 1.96%. These good results stem from the fact that the sinusoidal assumption at the nonlinearity output is adequate, since the ratio of third harmonic to fundamental at this point is less than 10% for a wide range of K values.

The major difference between this example and Example 1 is that the cube root nonlinearity does not approach a linear characteristic as the oscillation amplitude becomes large or small. Therefore, there is no tendency, for large or small K, for the DF and rms DF approximations to become exact.

4.3 EXAMPLE 3

This system has the same high pass linear plant of Example 2, but the nonlinearity is now a preload with parameters defined in Fig. 4.11.

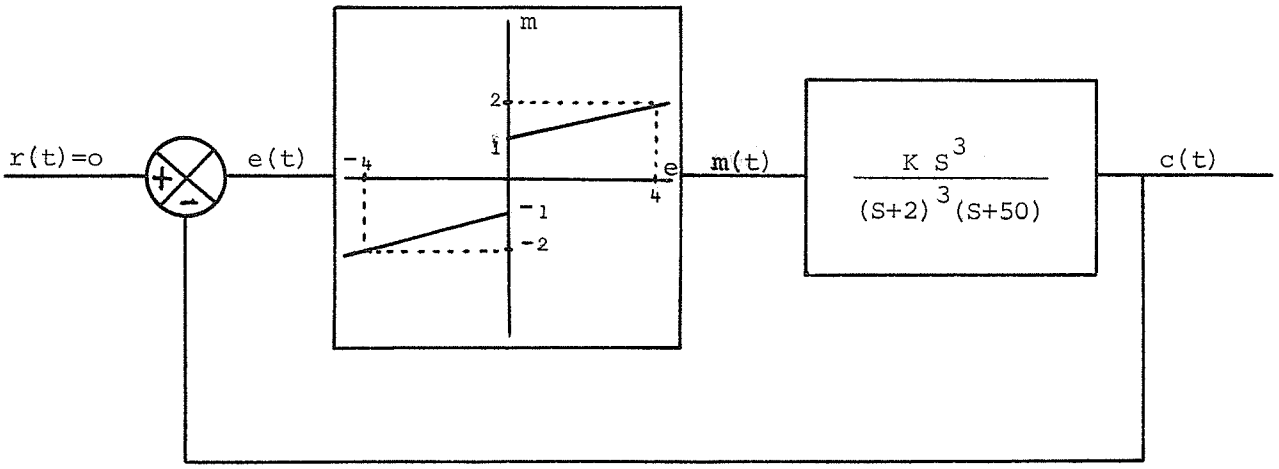

Fig. 4.11

CLOSED LOOP SYSTEM OF EXAMPLE 3

This system has the same theoretical fundamental frequency of oscillation of Example 2, as well as the same high pass characteristics. Refer to Fig. 4.7 and 4.8 for the frequency, amplitude loci and the Bode diagram for this system.

As in the previous examples, the direct and reverse DF and rms DF approximations were calculated for various values of gain K . The system was then simulated on the digital computer to determine the "exact" amplitudes of the fundamental component at these values of K .

The actual fundamental frequency of oscillation was 1.105 rad./sec. which was 2.6% below the theoretical value. As the gain K was increased, the frequency of oscillation slightly decreased and the amplitude of oscillation increased.

TABLE 5

DIRECT DF AND REVERSE DF, DIGITAL SIMULATION, EXAMPLE 3

K	E_D	Measured E	% Error in E	M_R	Measured M	% Error in M
50	0.1577	0.110	43.11	1.094	1.141	4.09
100	0.3254	0.243	34.17	1.161	1.140	1.77
300	1.1192	0.900	24.42	1.412	1.400	0.87
500	2.1856	1.740	25.58	1.710	1.593	7.32
1000	7.6570	6.826	12.17	3.133	2.911	7.64
1250	15.3353	14.633	4.80	5.074	4.931	2.90
1500	46.2621	43.902	5.37	12.825	12.245	4.78

TABLE 6

DIRECT rms DF AND REVERSE rms DF, DIGITAL SIMULATION, EXAMPLE 3

K	E_D	Measured E	% Error in E	M_R	Measured M	% Error in M
50	0.175	0.110	58.48	1.066	1.141	6.54
100	0.359	0.243	48.14	1.119	1.140	1.85
300	1.221	0.900	35.77	1.345	1.400	3.90
500	2.367	1.740	36.00	1.629	1.593	2.23
1000	8.011	6.826	17.36	3.021	2.911	3.80
1250	15.793	14.633	7.92	4.945	4.931	0.27
1500	46.865	43.902	6.75	12.707	12.245	3.77

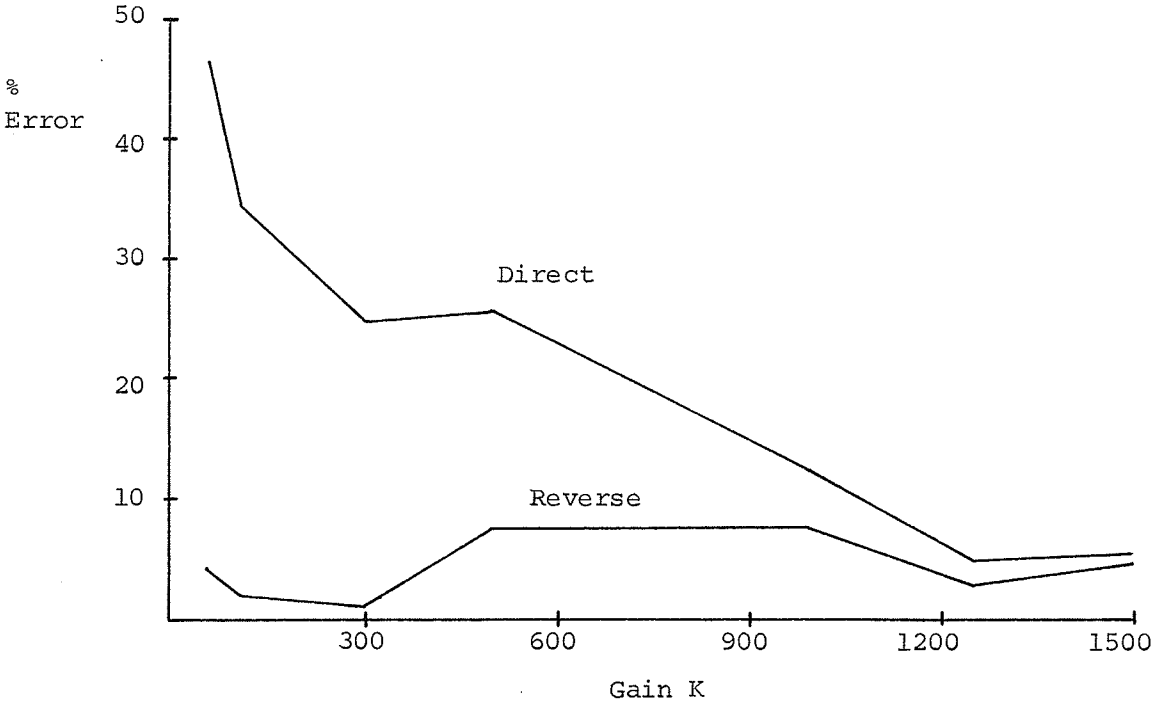

Fig. 4.12

ERRORS IN THE DIRECT AND REVERSE DF METHODS, EXAMPLE 3

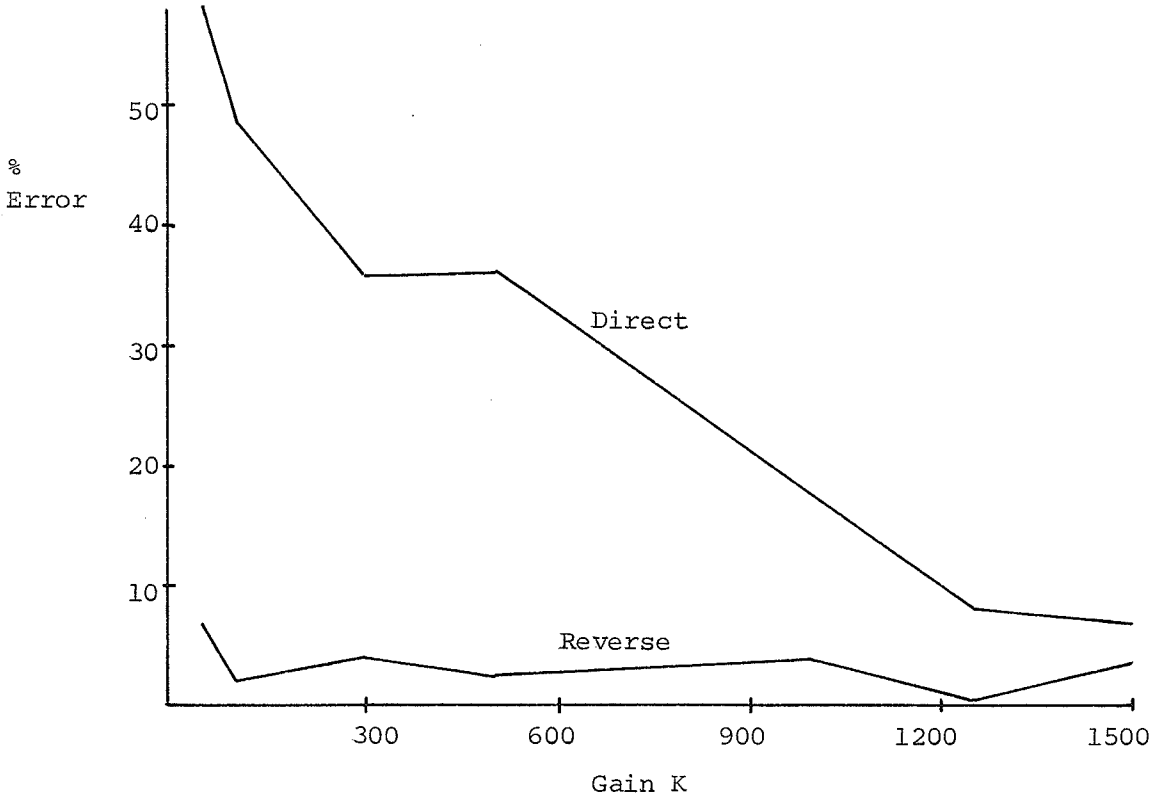

Fig. 4.13

ERRORS IN THE DIRECT AND REVERSE rms DF METHODS, EXAMPLE 3

The same general trend of the two previous examples is again prevalent here. The direct method approximations are very poor, with the maximum error in the DF case being 43.11% and in the rms DF case 58.48%. These errors are due to the high third harmonic content in the nonlinearity input - as much as 32% for small values of K .

The reverse method gives very good results, with the error in the DF case being less than 7.64% and in the rms DF case less than 6.54%. The third harmonic content in the nonlinearity output signal is less than 12% for all values of K tested, and hence the sinusoidal approximation at this point is quite good.

Because of the characteristic of the nonlinearity, small oscillation amplitudes have high harmonic content. This is reflected in the direct approximations, which have very large errors. As the oscillation magnitude becomes very large, the nonlinear characteristic becomes fairly linear and the direct and reverse approximations both become quite accurate. In this case, it is difficult to say that one method is more accurate than another.

4.4 COMMENTS

A system possessing a high pass linear plant can be accurately analyzed by means of the reverse DF and reverse rms DF. The reverse predictions were consistently close to the actual values. In each case, the harmonic content

at the nonlinearity output was much smaller than that at the nonlinearity input. The reverse method does not offer any improvement on the prediction of the frequency of oscillation, as both direct and reverse predict the same frequency.

Only three nonlinearities and two high pass plants have been analyzed, but the results are very encouraging. An important point is that mathematical inversion (Sec. 1.1.2) is born out by these physical results, even though the signal travels in a clockwise direction. By mathematically inverting the signal flow, a high pass system becomes low pass. This means that mathematically the reverse method retains the filter hypothesis of the direct DF method.

Although the reverse method works very well in these chosen examples, it cannot be assumed to hold in general unless a more thorough investigation of nonlinearities and high pass systems is made. These results make this method very desirable, but no doubt there are exceptions to which this method may not be applied.

In each example, it was observed that the reverse rms DF produced the most accurate approximation. This method deals with equivalent energy and hence includes harmonic content to a certain extent. This would be expected to produce better results than the reverse DF method, which only deals with the fundamental component.

CHAPTER 5

THE DIDF AND ITS CALCULATION

The Dual Input Describing Function (DIDF) is used to improve the DF by assuming two components at the nonlinearity input instead of the one sinusoid in the DF case. The input assumption may be a sinusoid plus bias, two sinusoids, or a sinusoid plus random noise [10 pp.402-420]. This thesis will deal only with the two sinusoid case (the two frequencies being commensurate). The nonlinearity output consists of a whole Fourier spectrum of signals, each frequency being a multiple (submultiple) of the two input frequencies. Only the two output components of the same frequency as the inputs will be considered, as the remainder are assumed to be eliminated by the low pass linear plant. The DIDF may also be used to predict oscillations with bias, determine limits for jump resonance, and predict and analyze subharmonic behaviour.

5.1 FORMULATION OF THE DIDF

The general autonomous nonlinear system of Fig. 3.1 will again be considered. The input to the nonlinearity is approximated by

$$e(t) = A \sin \omega t + B \sin(n\omega t + \phi) \qquad (5.1)$$

where ϕ is the phase shift between the two assumed wave-

forms. Usually, $n=3$ as the third harmonic is most prevalent.

There are now two equivalent gains to be considered, one for the fundamental component and one for the harmonic. These equivalent gains are both functions of A,B, ω, and ϕ, except in the case of static, single-valued nonlinearities where they are independent of frequency ω. For such a nonlinearity, the equivalent gain of the fundamental component is

$$N_1(A,B,\phi) = N_{1r}(A,B,\phi) + j\, N_{1i}(A,B,\phi) \qquad (5.2)$$

and of the harmonic component is

$$N_n(A,B,\phi) = N_{nr}(A,B,\phi) + j\, N_{ni}(A,B,\phi) \qquad (5.3)$$

where

$$N_{1r}(A,B,\phi) \equiv \frac{1}{\pi A}\int_0^{2\pi} f(A\sin u + B\sin(n u + \phi))\sin u\, du \qquad (5.4)$$

$$N_{1i}(A,B,\phi) \equiv \frac{1}{\pi A}\int_0^{2\pi} f(A\sin u + B\sin(n u + \phi))\cos u\, du \qquad (5.5)$$

$$N_{nr}(A,B,\phi) \equiv \frac{1}{\pi B}\int_0^{2\pi} f(A\sin u + B\sin(n u + \phi))\sin nu\, du \qquad (5.6)$$

$$N_{ni}(A,B,\phi) \equiv \frac{1}{\pi B}\int_0^{2\pi} f(A\sin u + B\sin(n u + \phi))\cos nu\, du \qquad (5.7)$$

The conditions for self oscillation in the system are determined by balancing each frequency component around the closed loop. The resulting two equations are:

$$N_1(A,B,\phi)G(j\omega) = -1 \tag{5.8}$$

and

$$N_n(A,B,\phi)G(jn\omega) = -1 \tag{5.9}$$

These relations are depicted graphically.

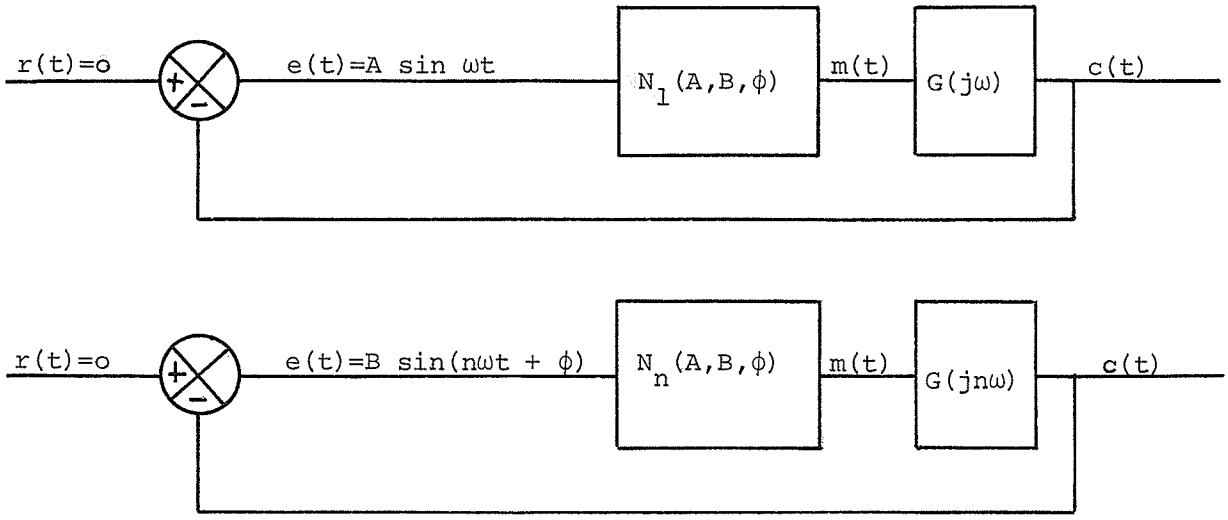

Fig. 5.1

LINEARIZED, CLOSED LOOP SYSTEM FOR DIDF

Each frequency component is balanced separately, but the equivalent gains are coupled to each other through the variables A,B, and ϕ .

Because of the complex nature of the equivalent gains, there will be four equations in the four unknowns A,B,ω , and ϕ . This set of simultaneous, nonlinear equations can be solved by the methods outlined in Chapter 2.

CHAPTER 6

APPLICATION OF THE REVERSE DIDF

The reverse DIDF will be applied to a specific example using the techniques outlined in the previous chapters. The predictions based on this method will be compared with the direct and reverse DF and the direct DIDF predictions, and with the actual values obtained through simulation. A discussion is included on the accuracy of the DIDF as related to the DF.

6.1 EXAMPLE 4

This example may be termed a contrived system, as the linear plant equally attenuates the fundamental and third harmonic. All the higher harmonics are sufficiently attenuated to be ignored. This presents an ideal situation for application of the DIDF, as the resultant waveform is composed of essentially two sinusoids - the fundamental frequency and its third harmonic. The nonlinearity was the odd square root: $m = |e|^{\frac{1}{2}} \operatorname{sgn} e$.

The fundamental frequency of oscillation, as found by the DF method in Fig. 6.2, is 1.28532 rad./sec. The third harmonic will have a frequency of 3.85596 rad./sec. The Bode diagram of the bandpass linear plant is shown in Fig. 6.3.

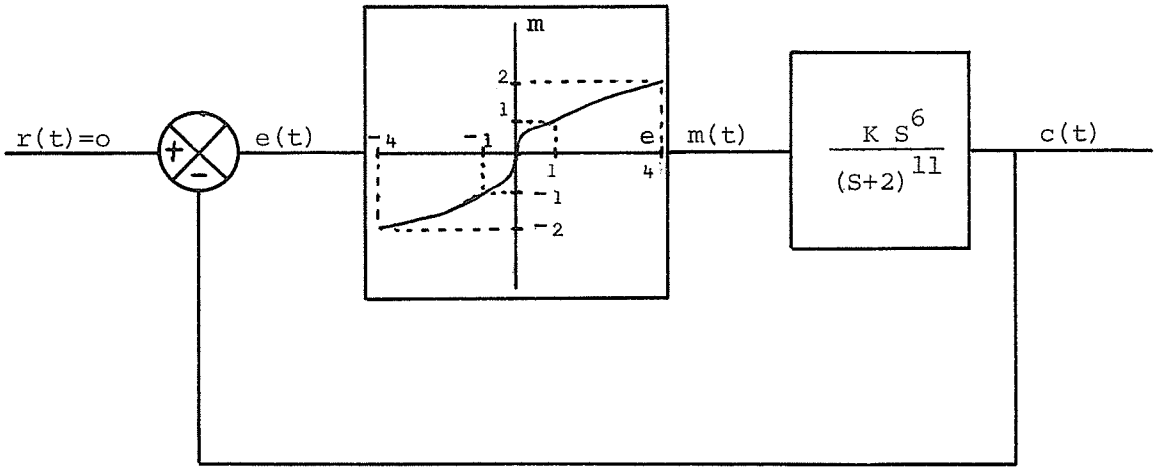

Fig. 6.1

CLOSED LOOP SYSTEM OF EXAMPLE 4

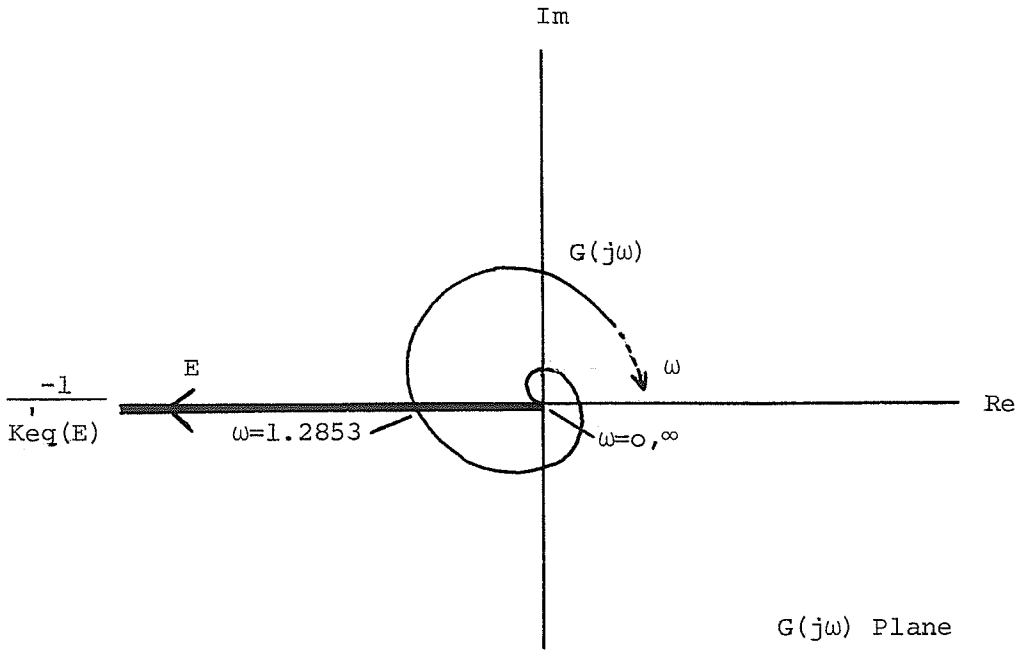

Fig. 6.2

FREQUENCY AND AMPLITUDE LOCI, EXAMPLE 4

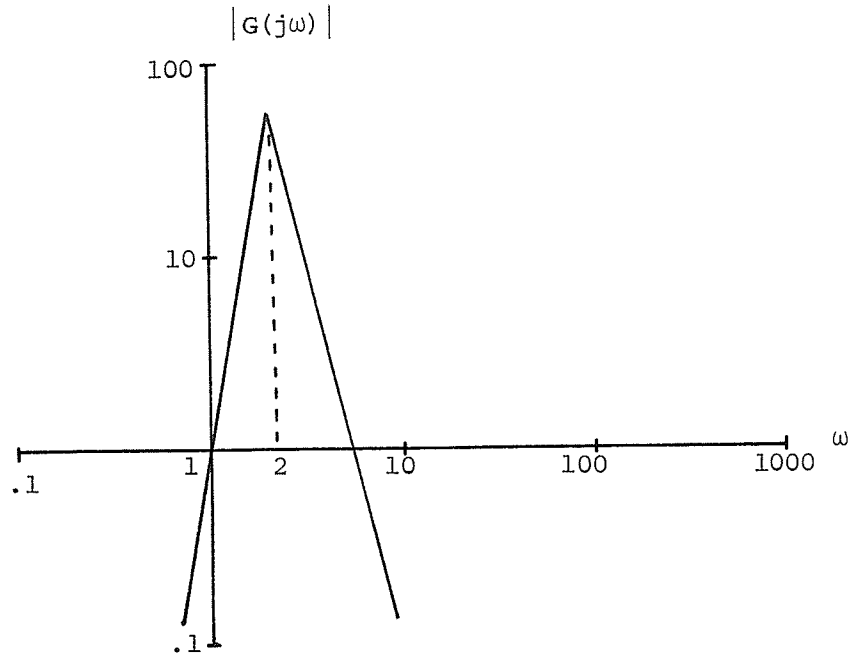

Fig. 6.3

BODE DIAGRAM OF BANDPASS SYSTEM, EXAMPLE 4

The DIDF predictions were found using the pattern search optimization routine and the system was simulated on the digital computer. In the direct case, the nonlinearity input was approximated by $e(t) = A\sin \omega t + B \sin (3\omega t + \phi)$ and in the reverse case the nonlinearity output was approximated by $m(t) = A\sin \omega t + B \sin(3\omega t + \phi)$.

The actual fundamental frequency of oscillation was 1.283 rad./sec., which was only 0.18% below the DF predicted frequency.

The direct and reverse DF methods gave similar results, due to the chosen linear plant. This plant attenuates the fundamental and third harmonic components equally, and hence the harmonic content at the input and output of the nonlinearity is about the same. For each of the values

TABLE 7

DIRECT DF AND DIRECT DIDF, DIGITAL SIMULATION, EXAMPLE 4

K	DF			DIDF		
	E_D	Meas'd E	% Error in E	Pred'd E	Meas'd E	% Error in E
2500	0.8325	0.888	6.19	0.7828	0.888	11.95
5000	33.3300	3.520	5.40	3.145	3.520	10.65
7500	7.4926	7.983	6.14	7.041	7.983	11.77
10000	13.3203	14.267	6.58	13.27	14.267	6.94
14000	26.1075	27.580	5.35	24.76	27.580	10.23
18000	43.1573	45.952	6.08	40.59	45.952	11.65

TABLE 8

REVERSE DF AND REVERSE DIDF, DIGITAL SIMULATION, EXAMPLE 4

K	DF			DIDF		
	M_R	Meas'd M	% Error in M	Pred'd M	Meas'd M	% Error in M
2500	0.9684	1.047	7.54	1.040	1.047	0.71
5000	1.9368	2.085	7.09	2.079	2.085	0.26
7500	2.8455	3.140	9.39	3.118	3.140	0.65
10000	3.8736	4.197	7.72	4.159	4.197	0.88
14000	5.4230	5.834	7.05	5.818	5.834	0.25
18000	6.9724	7.534	7.45	7.483	7.534	0.71

NOTE: E_D, M_R and % ERROR are following the same convention as in Chapter 4.

of gain K used, the third harmonic content at the nonlinearity input was about 21% and at the nonlinearity output about 23%. This means that the sinusoidal approximation at the nonlinearity input is slightly better than at the output, and this slight difference is reflected in the errors resulting from these approximations. The direct DF case has an error slightly over 6%, while the reverse DF errs by slightly over 7%. This is a clear example of how harmonic imbalance at the input and output of the nonlinearity plays an important role in deciding which method will result in the best approximation.

The direct and reverse DIDF are very poor and very good respectively. The direct DIDF produces a worse approximation to the fundamental component than the direct DF. This is contrary to expectations, as the DIDF was introduced as an improvement to the DF. This apparent contradiction is investigated in the next section. On the other hand, the reverse DIDF predictions are very accurate, erring from the actual by less than 0.88% for all the values of K used. Because of the high pass(or bandpass)nature of the linear plant, the reverse method was expected to be more accurate, and this was born out by physical experiment.

The nonlinearity does not become approximately linear for large or small inputs, and hence neither the direct or reverse methods will become exact. This is reflected in the relatively constant errors between prediction and actual for all values of K used.

6.2 ACCURACY OF THE DIDF

The DIDF was introduced to act as an improvement on the DF, but in the direct case of Example 4 the DIDF approximation was worse. This result was unexpected, but reflects the uncertainty involved when dealing with non-linear systems. This may be a common phenomena, or the chosen example may be one of the exceptions to the rule.

The DF method involves finding the minimum of a two dimensional surface, but the DIDF immediately changes the problem to four dimensions. In order to get an idea of the process of finding the absolute minimum in the DF or DIDF case, a contour study was performed on the system of Example 4. Contours were drawn for constant values of the norm of eqn. 2.2, the absolute minimum being located where the norm equals zero. The labelled contours of Figs. 6.4-6.7 indicate the value of the norm or residual. The contours were drawn as a function of the DF variables A and ω. The contour of Fig. 6.4 shows the approximate location of the DF solution while the DIDF solution contours are in Fig. 6.5 (using as fixed parameters the B and ϕ values of the actual DIDF solution). To see how the DIDF solution shifts as the third harmonic B and phase shift ϕ variables are changed from the actual DIDF solution, two more contours were drawn. Fig. 6.6 shows the contour map of the DIDF solution with B decreased 5% and ϕ decreased 6.25% from the actual DIDF solution. A 10% decrease in B and

a 12.5% decrease in ϕ from the actual DIDF solution produced the contour map of Fig. 6.7. From simulation, the actual nonlinearity input waveform had an amplitude of 3.52 at a frequency of 1.283 rad./sec.

It can be easily observed that the approximate DF solution is closer to the actual values than the DIDF solution. Hence, as was previously stated, the DF is more accurate than the DIDF. The main purpose of these figures is to show that the third harmonic and phase shift have a pronounced effect on the contours of the DIDF solution, and hence on the location of the minimum. Fig. 6.6 shows that the contours have been altered so that two minima appear to exist, both being local minima, or one being a local minimum and one the absolute minimum. This raises the question that perhaps the optimization routine used in Example 4 was converging on a local minimum nearby to the absolute minimum, as this computer program does not guarantee the absolute minimum. This fact could explain why the direct DIDF was not as accurate as the direct DF.

This points out one of the major difficulties involved when dealing with a four dimensional nonlinear problem. The actual four dimensional contours are far more complex than those in Figs. 6.5-6.7 and at times the results may not meet expectations (ie. DIDF more accurate than DF). In these cases the absolute minimum could possibly be found by applying other mathematical techniques. Therefore, the

accuracy of the DIDF is largely indeterminant, due to the uncertainty as to which kind of minimum has been found.

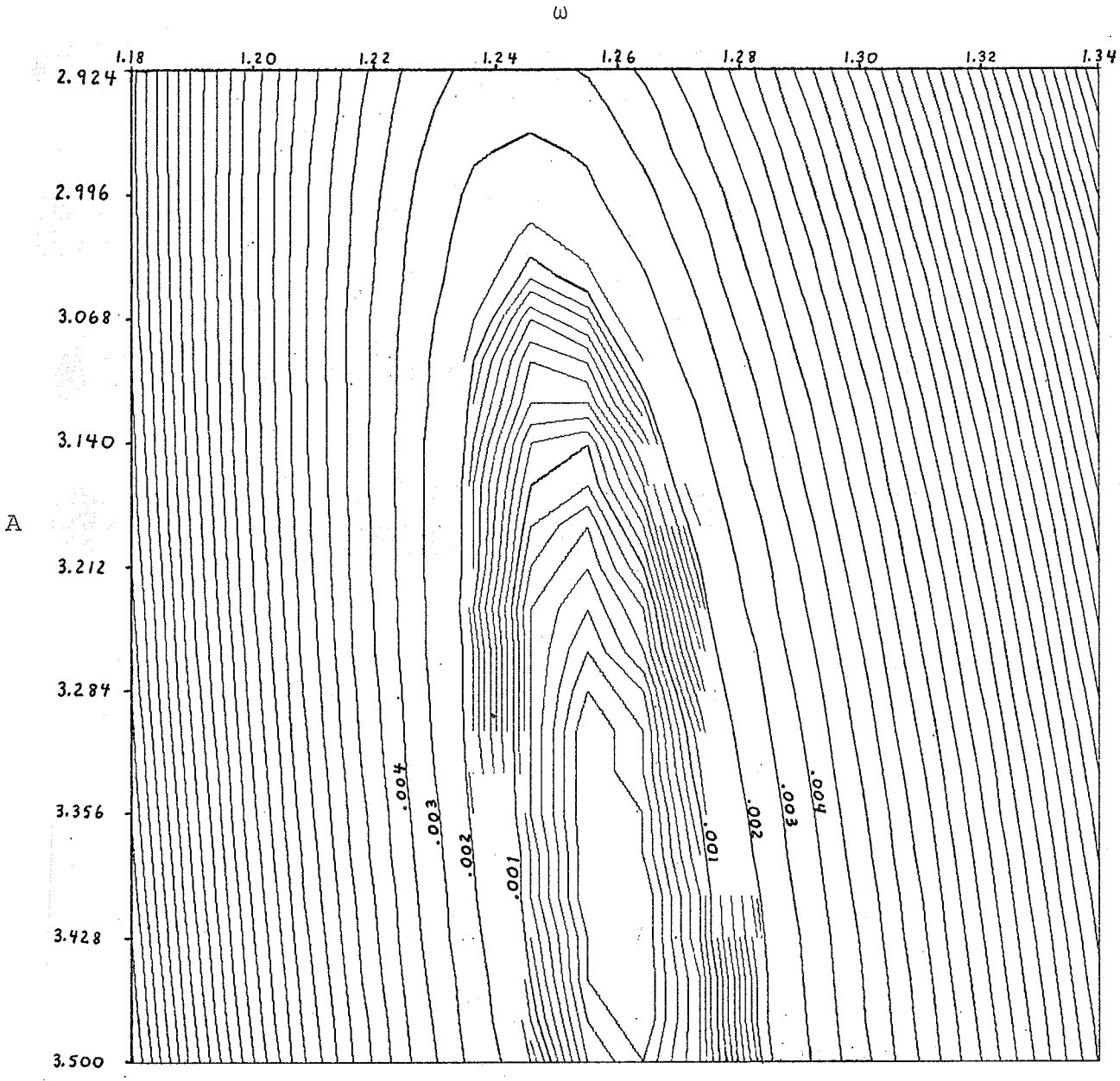

Fig. 6.4

CONTOUR MAP OF DF SOLUTION

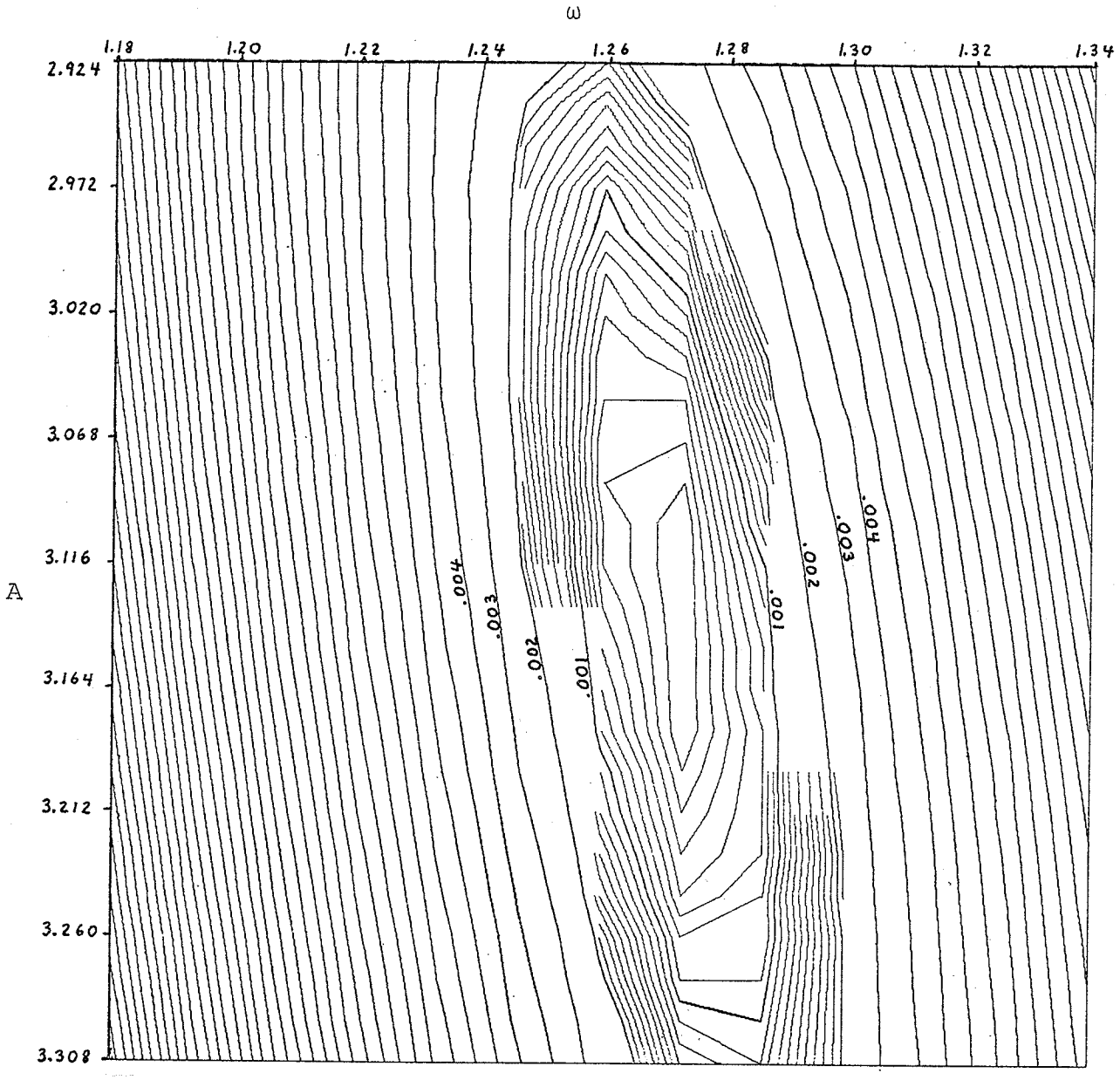

Fig. 6.5

CONTOUR MAP OF DIDF SOLUTION

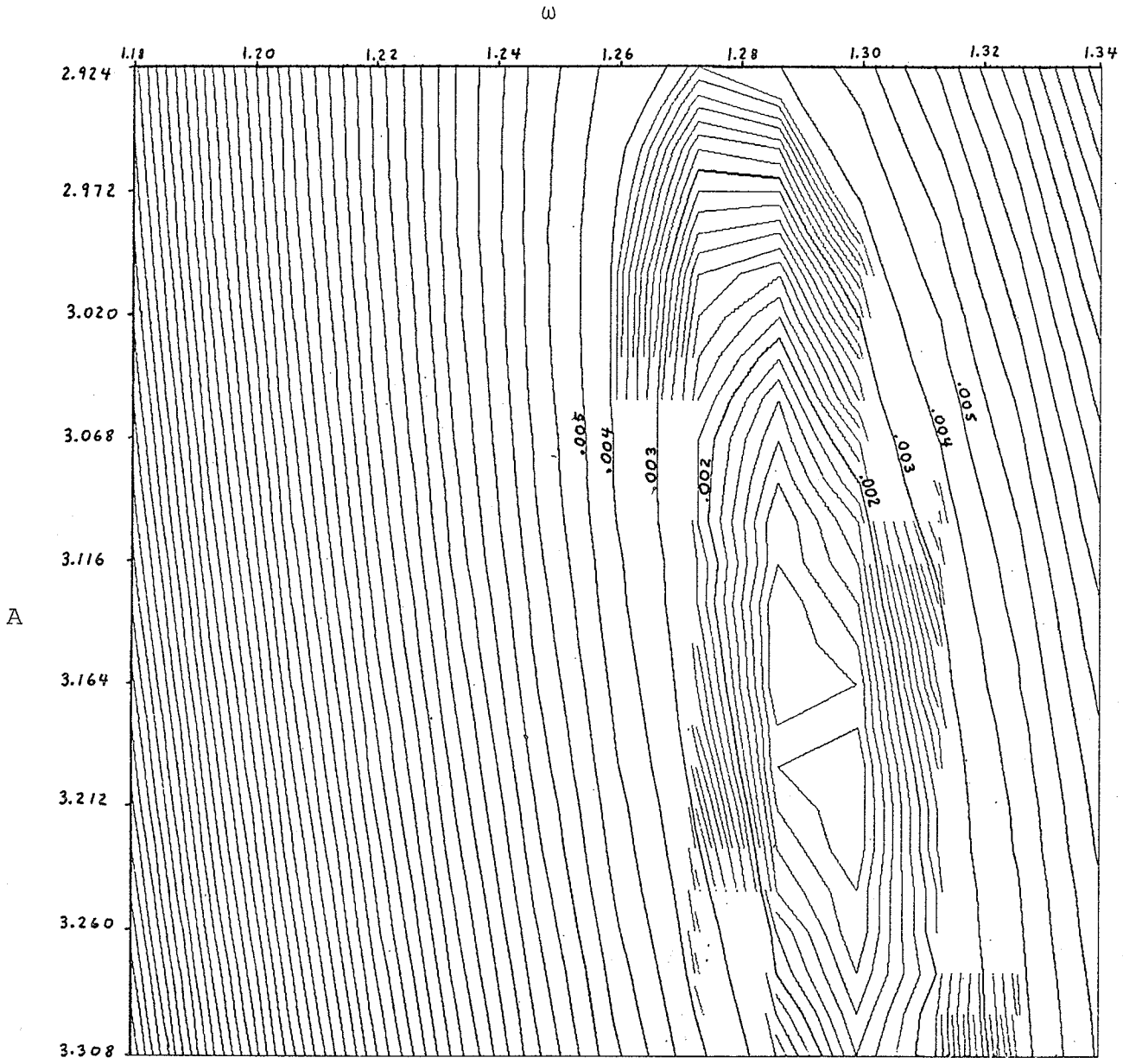

Fig. 6.6

CONTOUR MAP OF DIDF SOLUTION
WITH B DECREASED 5% AND ϕ DECREASED 6.25%
FROM ACTUAL DIDF SOLUTION

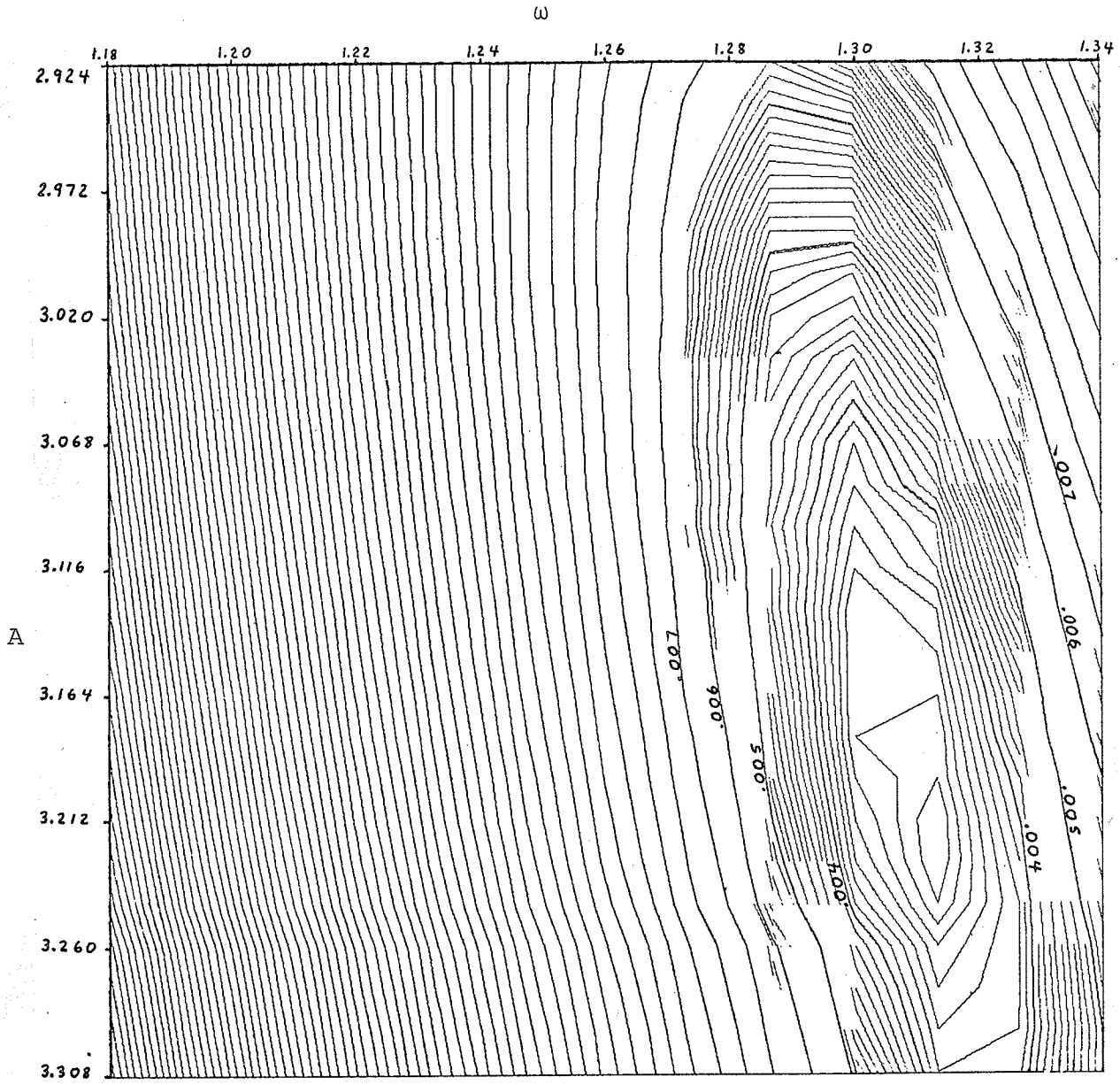

Fig. 6.7

CONTOUR MAP OF DIDF SOLUTION

WITH B DECREASED 10% AND ϕ DECREASED 12.5%

FROM ACTUAL DIDF SOLUTION

CHAPTER 7

JUMP PHENOMENA PREDICTION

The describing function approach can be extended to study the behaviour of a closed loop nonlinear system under a specified excitation. Jump resonance is one of the common phenomena exhibited in nonlinear control systems. It is observed in some nonlinear systems under a periodic excitation that when the amplitude or period of the excitation is smoothly changed, the system output undergoes a discontinuous change in amplitude. In many cases this phenomenon is undesirable, thus making the prediction of jump resonance very important. The systems to be examined in the following sections exhibit no self-oscillation, making the response totally due to the forcing function. The jumps will be brought about by smoothly varying the excitation amplitude.

7.1 SINUSOIDAL DRIVING FUNCTION [14]

The example system chosen has a high pass linear plant and a gain changing nonlinearity as defined in Fig. 7.1.

The problem here is to predict at what amplitude of sinusoidal excitation the system response will undergo a discontinuous rise or fall in amplitude. Because a driving function has been introduced, the closed loop equations for the direct and reverse method will be slightly changed from

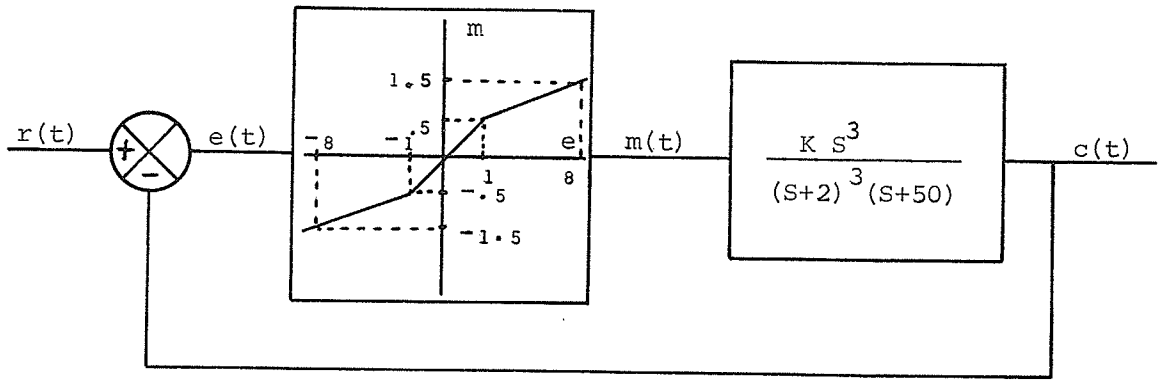

Fig. 7.1

SYSTEM FORCED BY SINUSOIDAL FUNCTION

eqns. 1.5 and 1.10. The closed loop equation for the direct DF method is

$$Re^{j\alpha} = E + E\ K'eq(E)\ G(j\omega) \qquad (7.1)$$

where $e(t) = E \sin \omega t$ and $r(t) = R \sin(\omega t + \alpha)$ and for the reverse DF method is

$$Re^{j\beta} = M\ R'eq(M) + M\ G(j\omega) \qquad (7.2)$$

where $m(t) = M \sin \omega t$ and $r(t) = R \sin(\omega t + \beta)$. $K'eq(E)$ and $R'eq(M)$ are the direct and reverse equivalent sinusoidal gains respectively for the static, single-valued nonlinearity, and are real. Since $G(j\omega)$ is complex, each equation may simply be solved by equating its real and imaginary parts. A typical input-output amplitude relation is shown in Fig. 7.2.

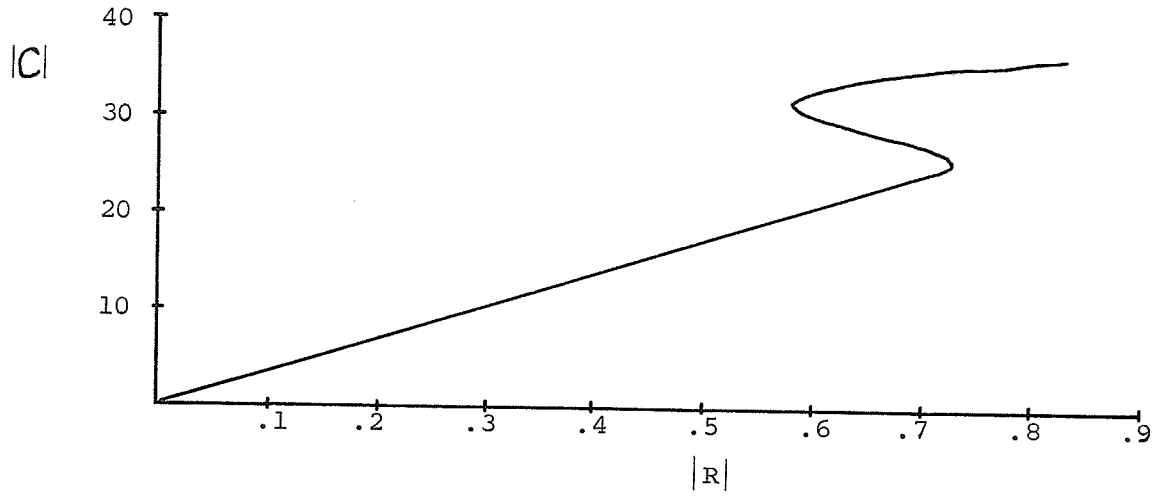

Fig. 7.2

INPUT-OUTPUT AMPLITUDE RELATION FOR
K=800, ω=1.3 RAD./SEC., USING THE REVERSE DF METHOD

Simulation was performed on the analog computer to obtain the actual amplitudes of the sinusoidal forcing function at which the system response experienced jump up and jump down discontinuities.

For every combination of gain and input frequency, the reverse DF method gives the best predictions of jump up and jump down points. This approach was expected to be more accurate, due to the high pass nature of the linear plant. The harmonics generated by the nonlinearity, and amplified by the linear plant, cause distortion of the nonlinearity input signal. As a result, the nonlinearity output signal is expected to be more sinusoidal than the nonlinearity input, hence justifying the use of the reverse method. The harmonic content of the nonlinearity input and output waveforms was not ascertained experimentally,

TABLE 9

DIRECT DF AND REVERSE DF, JUMP UP, ANALOG SIMULATION

K	ω	R_D*	R_R**	Actual R	%Error in R_D	%Error in R_R
700	1.3	0.2430	0.4752	0.43	43.5	10.5
700	1.4	0.4852	0.9313	0.74	51.3	25.9
750	1.2	N.J.P.	0.1566	0.22	-	28.8
750	1.3	0.3009	0.5910	0.50	39.8	18.2
800	1.2	0.1187	0.2367	0.24	50.6	1.38
800	1.3	0.3690	0.7255	0.61	39.4	19.2
800	1.4	0.6536	1.2550	0.97	32.6	29.4
800	1.5	N.J.P.	N.J.P.	N.J.D.	-	-

N.J.P. = No Jump Predicted; N.J.D. = No Jump Detected

*R_D - Excitation amplitude prediction using the direct DF.

**R_R - Excitation amplitude prediction using the reverse DF.

TABLE 10

DIRECT DF AND REVERSE DF, JUMP DOWN, ANALOG SIMULATION

K	ω	R_D	R_R	Actual R	%Error in R_D	%Error in R_R
700	1.3	0.2426	0.4621	0.41	40.8	12.7
700	1.4	0.4846	0.9129	0.72	48.5	26.8
750	1.2	N.J.P.	0.1563	0.175	-	10.7
750	1.3	0.2790	0.5252	0.48	41.9	9.4
800	1.2	0.0940	0.1786	0.215	56.4	16.9
800	1.3	0.3146	0.5906	0.55	44.6	7.4
800	1.4	0.6201	1.1647	0.94	34.0	23.9
800	1.5	N.J.P.	N.J.P.	N.J.D.	-	-

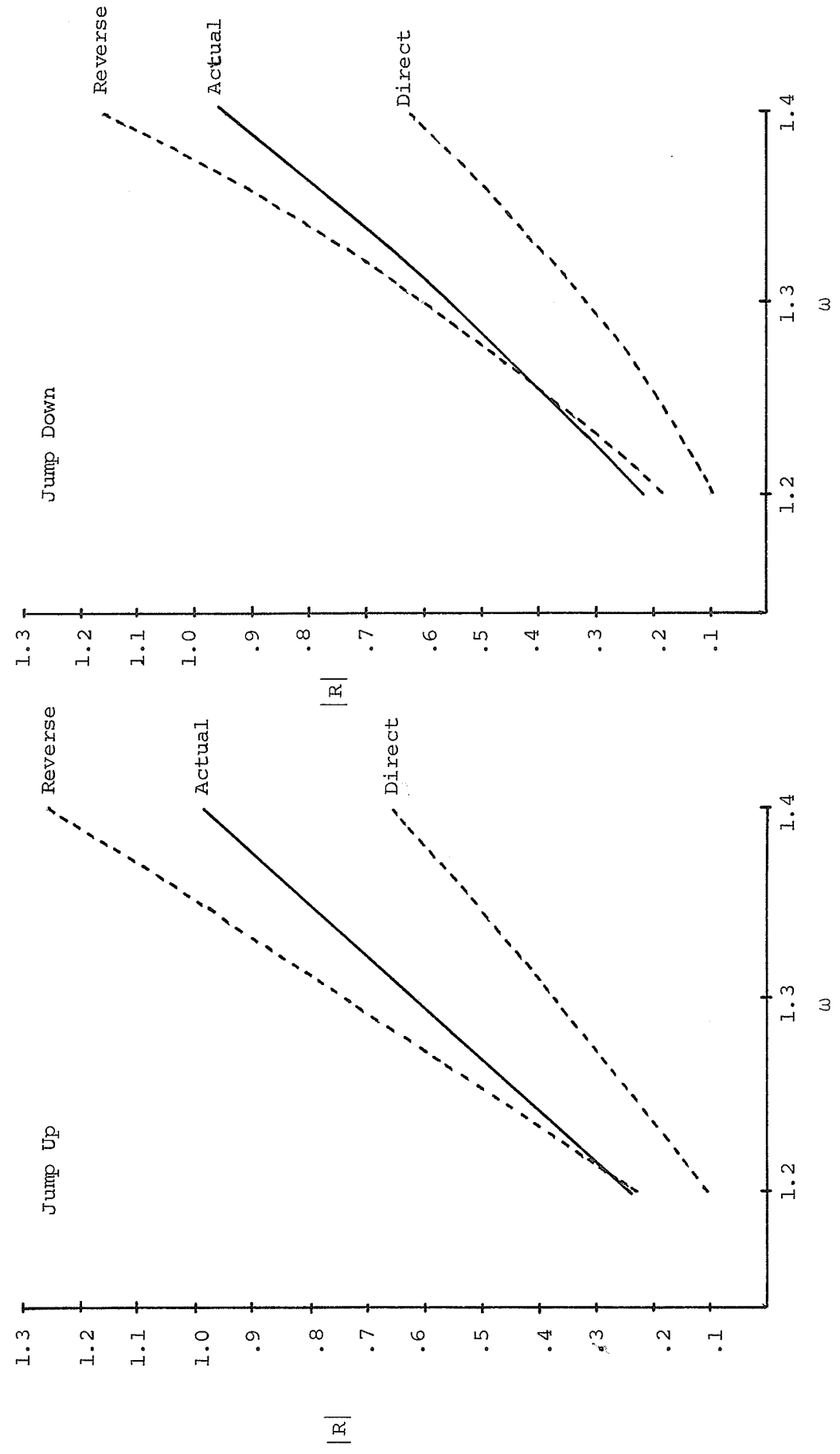

Fig. 7.3

PLOT OF JUMP-RESONANCE RESULTS FOR K=800

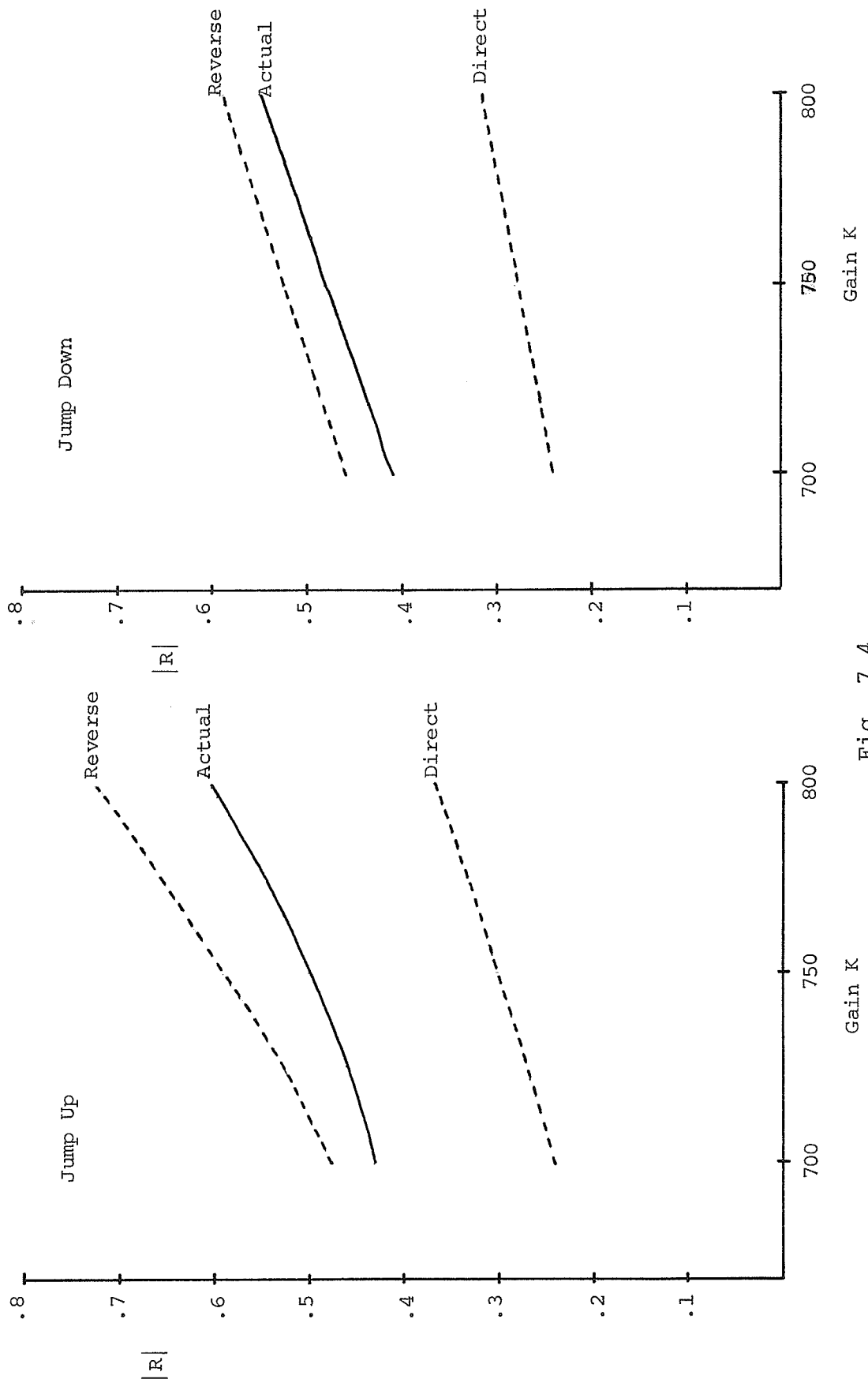

Fig. 7.4

PLOT OF JUMP RESONANCE RESULTS FOR EXCITATION FREQUENCY ω=1.3 RAD./SEC.

but the above reasoning would be expected to be borne out.

It is known that jump resonance can occur in a nonlinear control system if the vector locus of the linear plant passes through a certain region which depends only upon the nonlinear part [15]. A. Fukuma and M. Matsubara [15] further investigated the boundary curves of these regions and found that they are defined by certain equations as the envelope of the union of a large number of circles. This approach, related to the direct DF, may be applied to the reverse DF with only a few minor changes. Following the method of ref. 15 the resultant equation, pertaining now to the reverse DF, is

$$R \frac{\partial R}{\partial M} = M \left\{ \left(h_1 + \frac{\gamma_1 + n_1}{2} \right)^2 + \left(h_2 + \frac{\gamma_2 + n_2}{2} \right)^2 - \frac{(n_1 - \gamma_1)^2 + (n_2 - \gamma_2)^2}{4} \right\} \qquad (7.3)$$

where $\gamma_1 = n_1 + M \frac{\partial n_1}{\partial M}$ $\quad R'eq(M) = n_1(M) + j\, n_2(M)$

$\gamma_2 = n_2 + M \frac{\partial n_2}{\partial M}$ $\quad G(j\omega) = h_1(\omega) + j\, h_2(\omega)$ $\qquad (7.4)$

A region in which jump resonance may occur is associated with $\frac{\partial R}{\partial M} < 0$. The application of eqn. 7.3 follows the same format as in ref. 15. For a high pass system it is expected that the boundaries specified by eqn. 7.3 would be more accurate than those specified when using the direct DF approach equations of ref. 15.

7.2 TRIANGULAR DRIVING FUNCTION

This next example was chosen in an attempt to apply the reverse DF method to a different type of problem. Until now, this method has been applied to high pass systems, with the expectation that the nonlinearity output signal is more sinusoidal than the nonlinearity input signal, and hence the reverse approach should be more accurate. This example will attempt to justify the reverse method for a low pass plant and a triangular forcing function. The rationale behind this idea is that, for a smoothing type of nonlinearity, the nonlinearity output may be more sinusoidal than the nonlinearity input, which is a combination of a triangular excitation and a nearly sinusoidal feedback signal. If this is so, the reverse DF approach should result in better predictions. This idea was applied to the following example.

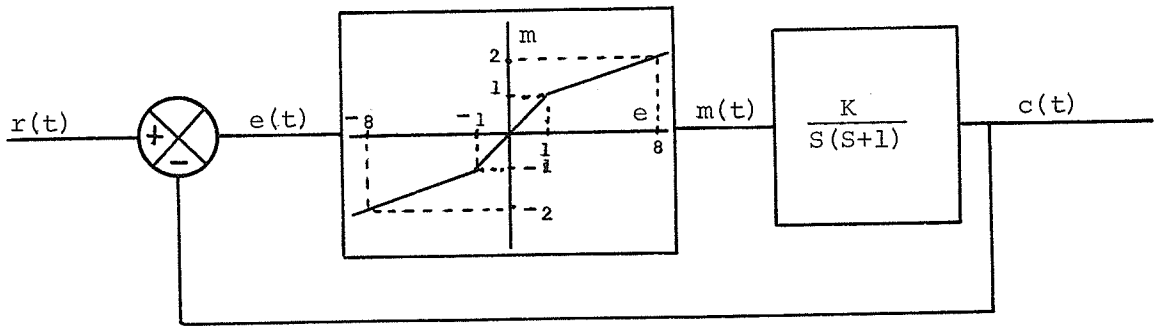

Fig. 7.5

SYSTEM CHOSEN TO OBSERVE JUMP PHENOMENON WITH TRIANGULAR FORCING FUNCTION

This system was simulated on the analog computer, and a Fourier analysis of $e(t)$, $m(t)$, and $r(t)$ was performed using the method proposed by Fifer [4]. Discontinuous jumps in the system output were achieved by slowly varying the amplitude of the triangular excitation $r(t)$ at a fixed frequency. The direct and reverse predictions of the jump points, in terms of a sinusoidal driving function, were found using eqns. 7.1 and 7.2. At the instant of any jump in the system response the triangular forcing function was fed into the Fourier analyzer to determine the magnitude of its fundamental component. This value was compared with the direct and reverse predictions to obtain a measure of error.

General trends are evident from these results. In all but one case the direct method is more accurate in predicting the jump up, and the jump down is best predicted by the reverse method in all but one case. An attempt will be made to justify these results. As the direct method is more accurate for predicting the jump up, it would be expected that just prior to the jump the nonlinearity input would be more sinusoidal than the nonlinearity output. In a similar fashion, the nonlinearity output would be expected to be more sinusoidal than the nonlinearity input, just prior to the jump down.

TABLE 11

DIRECT DF AND REVERSE DF, JUMP UP, ANALOG SIMULATION

K	ω	R_D*	R_R**	Actual R***	%Error in R_D	%Error in R_R
20	2.25	3.100	2.823	3.125	0.80	9.66
20	2.50	2.296	2.115	2.265	1.37	6.62
20	2.75	1.713	1.600	1.667	2.76	4.02
20	3.00	1.277	1.209	1.230	3.82	1.71
30	2.50	4.136	3.762	4.275	3.25	12.00
30	2.75	3.182	2.901	3.260	2.39	11.00
30	3.00	2.476	2.280	2.510	1.35	9.17
30	3.25	1.938	1.805	1.940	0.10	6.96
30	3.50	1.518	1.431	1.495	1.54	4.28

TABLE 12

DIRECT DF AND REVERSE DF, JUMP DOWN, ANALOG SIMULATION

K	ω	R_D	R_R	Actual R	%Error in R_D	%Error in R_R
20	2.25	2.793	2.629	2.625	6.40	0.15
20	2.50	1.904	1.780	1.775	7.27	0.28
20	2.75	1.349	1.249	1.225	10.12	1.96
20	3.00	0.988	0.907	0.893	10.63	1.57
30	2.50	3.808	3.630	3.810	0.05	4.72
30	2.75	2.603	2.475	2.460	5.82	0.61
30	3.00	1.840	1.736	1.650	11.51	5.21
30	3.25	1.348	1.260	1.232	9.42	2.27
30	3.50	1.019	0.944	0.924	10.28	2.17

*R_D - Excitation amplitude prediction (sinusoidal) using the direct DF.

**R_R - Excitation amplitude prediction (sinusoidal) using the reverse DF.

***Actual R - Amplitude of the fundamental component of the triangular forcing function at instant of jump.

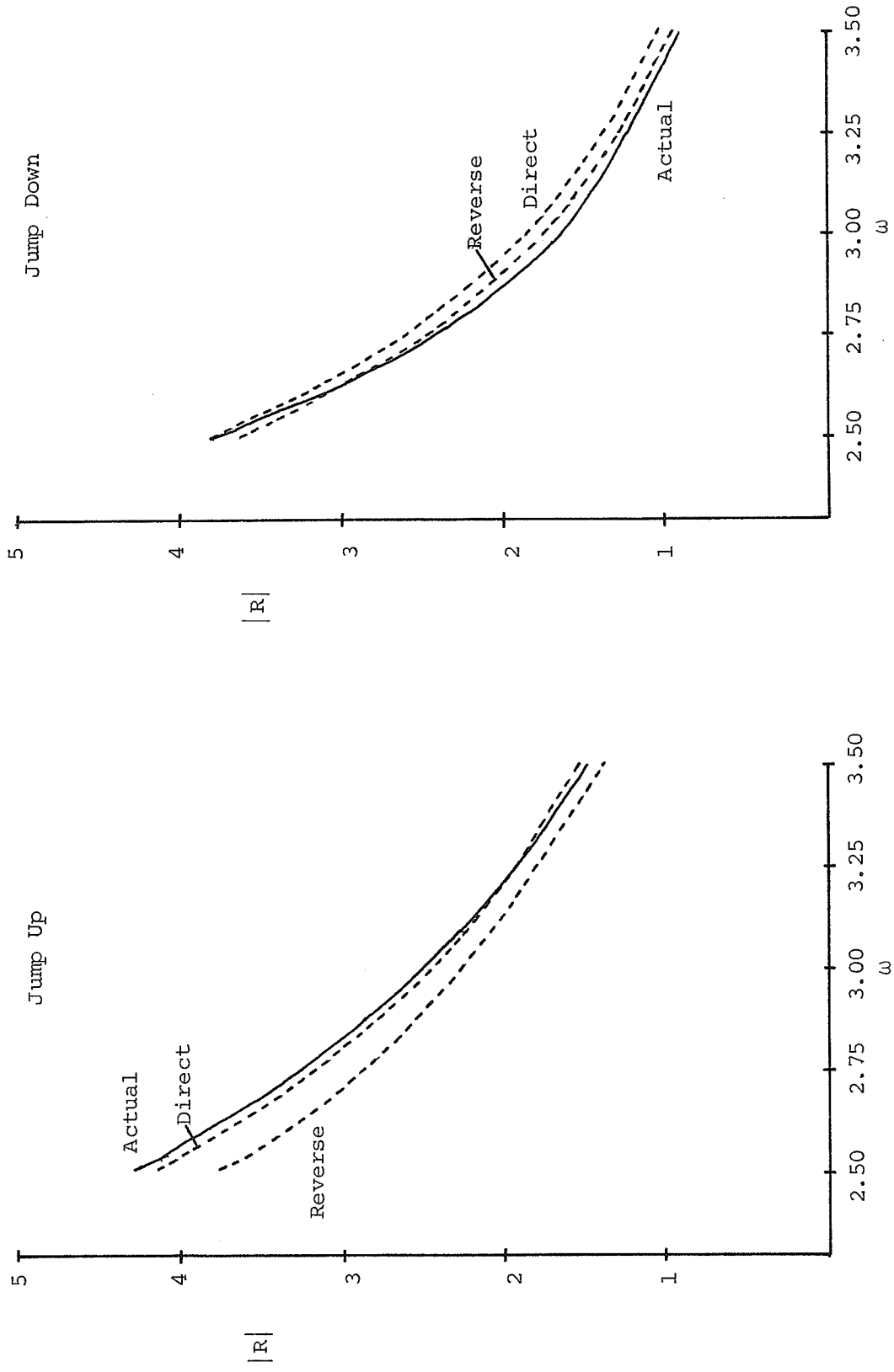

Fig. 7.6

PLOT OF JUMP RESONANCE RESULTS FOR K=30

A type of mean square (MS) error may be used to determine how sinusoidal a waveform is. The MS of the waveform and its fundamental component are found and a measure of error is defined as:

$$MS_{error} = \frac{MS_{waveform} - MS_{fund.comp.}}{MS_{waveform}} \times 100\% \qquad (7.5)$$

Just before the system response exhibited a discontinuity, the MS values of the nonlinearity input and output waveforms and the MS values of their fundamental components were found. These results have been tabulated.

TABLE 13

MS ERROR AT NONLINEARITY INPUT AND OUTPUT, JUMP UP

K	ω	MS_w* Input	MS_f** Input	% Error Input	MS_w Output	MS_f Output	% Error Output
20	2.5	1.89	1.815	3.97	0.888	0.858	3.38
20	3.0	0.80	0.792	1.00	0.597	0.588	1.51
30	3.0	1.825	1.764	3.34	0.842	0.806	4.28
30	3.5	0.88	0.841	4.44	0.673	0.652	3.05

*MS_w - Mean square value of the nonlinearity input (or output) waveform.

**MS_f - Mean square value of the fundamental component of the nonlinearity input (or output).

TABLE 14

MS ERROR AT NONLINEARITY INPUT AND OUTPUT, JUMP DOWN

K	ω	MS_w Input	MS_f Input	% Error Input	MS_w Output	MS_f Output	% Error Output
20	2.5	10.62	10.65	0.20	1.587	1.494	5.93
20	3.0	7.04	7.01	0.50	1.395	1.311	6.02
30	3.0	19.24	19.13	0.56	2.035	1.912	5.24
30	3.5	5.56	5.55	0.22	1.270	1.213	4.48

The error in the nonlinearity input and output, for the jump up case, is approximately the same and hence neither signal can be said to be more sinusoidal. This means that the direct and reverse predictions should be equally accurate. In the jump down case, the nonlinearity input has much less harmonic content than the output, and therefore the direct method should give the more accurate predictions. These results do not support the expectations that were outlined earlier.

This discrepancy does not mean that the theory built up in the preceding chapters has fallen apart. It just means that, in this case, the mean square error may not be the best way of comparing the nonlinearity input and output waveforms. In other chapters, the ratio of third harmonic to fundamental was used as a guide for determining which waveform (nonlinearity input or output) was more

sinusoidal. Perhaps if this measure, or any other, were used in this example one might get correlation between expectation and actual.

The applicability of the reverse method to low pass systems, in certain situations, is likely to result in accurate predictions but more work is required in this aspect.

CHAPTER 8

CONCLUSIONS

The describing function method may now be applied to a low or high pass system, with a reasonable expectation of good accuracy. The reverse method has retained the simplicity and generality of the original direct method. The major obstacles encountered were the solutions of the direct and reverse DIDF equations. Various high pass systems and nonlinearities were chosen, but the pattern search invariably converged to a local minimum instead of the exact solution. This could possibly be overcome by using different optimization routines.

This investigation has provided many avenues for future work. The reverse method has only been barely introduced and no limitations to its application have yet been tabulated. It has yet to be applied to the estimation of subharmonics. The idea of harmonic imbalance should be further investigated so as to develop a general rule as to when to use the direct or reverse method.[91] From the work described so far, a possible general rule would be : Determine the actual fundamental component and the most significant harmonic component of the nonlinearity input and output waveforms. Assume a sinusoid at the point where the ratio of harmonic to fundamental is least, and apply the appropriate method.[91] The DIDF problem led to the question

of DIDF accuracy as compared with DF accuracy. A further study should be done in this area to determine why, in some cases, a DIDF approximation is worse than a DF approximation.

REFERENCES

[1] Gelb, A., and W.E. Vander Velde, Multiple-Input Describing Functions and Nonlinear System Design. New York: McGraw-Hill Book Company, Inc., 1968.

[2] Truxal, John G., Automatic Feedback Control System Synthesis. New York: McGraw-Hill Book Company, Inc., pp. 88-160, 1955.

[3] Mason, S.J., "Feedback Theory - Some Properties of Signal Flow Graphs," Proc. I.R.E., Vol. 41, pp. 1144-1157, September 1953.

[4] Fifer, Stanley, Analogue Computation, Theory, Techniques and Applications. New York: McGraw-Hill Book Company, Inc., pp. 966-970, 1961.

[5] Protter, Murray H., and Charles B. Morrey, Jr., Modern Mathematical Analysis. Reading, Massachussettes: Addison-Wesley Publishing Company, Inc., p. 172, 1964.

[6] Carnahan, Brice, H.A. Luther and James O. Wilkes, Applied Numerical Methods. New York: John Wiley and Sons, Inc., 1969.

[7] Hooke, Robert, and T.A. Jeeves, "Direct Search Solution of Numerical and Statistical Problems," J.A.C.M., Vol. 8, pp.212-229, 1960.

[8] Macdonald, P.A., "Locating the Minimum of a Function by Pattern Search," Department of Electrical Engineering Publications, 69-TR12, NAG-011, Winnipeg:

University of Manitoba, April 1969.

[9] Beckett, R., and J. Hurt, Numerical Calculations and Algorithms. New York: McGraw-Hill Book Company, Inc., p.62, 1967.

[10] Gibson, John E., Nonlinear Automatic Control. New York: McGraw-Hill Book Company, Inc., p.381, 1963.

[11] Gibson, J.E., and K.S. Prasanna-Kumar, "A New RMS Describing Function for Single-Valued Nonlinearities," Proc. I.R.E., Vol. 49, p.1321, August 1961.

[12] Gille, J-C., M.J. Pelegrin and P. Decaulne, Feedback Control Systems. New York: McGraw-Hill Book Company, Inc., pp.419-421, 1959.

[13] Leach, Barry W., "An Evaluation of Estimates of Stability of Oscillations in Nonlinear Systems," Ph.D. Thesis, Dept. of Electrical Engineering, University of Manitoba, pp.25-27, February 1972.

[14] Hsu, Jay C., and Andrew U. Meyer, Modern Control Principles and Applications. New York: McGraw-Hill Book Company, Inc., pp.217-224, 1968.

[15] Fukuma, A., and M. Matsubara, "Jump Resonance Criteria of Nonlinear Control Systems," IEEE Trans. on Automatic Control, Vol. AC-11, No. 4, pp.699-706, October 1966.